1972

MSUCL-33
COO-1779-53

The Decay of ^{141m}Sm – A Three-Quasiparticle Multiplet in ^{141}Pm

R. E. Eppley
Department of Chemistry and Cyclotron Laboratory,
Department of Physics,

R. R. Todd
Cyclotron Laboratory, Department of Physics,

R. A. Warner and Wm. C. McHarris
Department of Chemistry and Cyclotron Laboratory,
Department of Physics,

and

W. H. Kelly
Cyclotron Laboratory, Department of Physics

Cyclotron Laboratory
Michigan State University

MSUCL-33
COO-1779-53

The Decay of ^{141m}Sm — A Three-Quasiparticle Multiplet in ^{141}Pm

R. E. Eppley*

Department of Chemistry† and Cyclotron Laboratory,‡ Department of Physics,

R. R. Todd

Cyclotron Laboratory,‡ Department of Physics,

R. A. Warner and Wm. C. McHarris

Department of Chemistry† and Cyclotron Laboratory,‡ Department of Physics,

and

W. H. Kelly

Cyclotron Laboratory,‡ Department of Physics

Michigan State University

East Lansing, Michigan 48823

Received_____

*Present address: Lawrence Radiation Laboratory, Berkeley, California 94720

†Work supported in part by the U.S. Atomic Energy Commission

‡Work supported in part by the U.S. National Science Foundation

Abstract:

We have studied the γ rays emitted following the decay of 22.1-min ^{141m}Sm with Ge(Li) and NaI(Tl) detectors in various singles, coincidence, and anticoincidence configurations, including Ge(Li)-Ge(Li) two-dimensional "megachannel" coincidence experiments. Of the 47 γ rays definitely established as belonging to ^{141m}Sm decay, all but six very weak ones have been placed in a consistent decay scheme. The energies [and J^{π} assignments] of the states in ^{141}Pm populated by the decay of ^{141m}Sm are 0 [$5/2^+$], 196.6 [$7/2^+$], 628.6 [$11/2^-$], 804.5 [$11/2^+$,$9/2^+$], (837.1) [$9/2^+$], 974.0 [$9/2^+$], 1108.1 [$7/2^+$,$9/2^+$,($5/2^-$)], 1167.2 [$13/2^{-(+)}$,$11/2^{-(+)}$,$9/2^{-(+)}$], 1313.2 [$13/2^{-(+)}$,$11/2^{-(+)}$,$9/2^{-(+)}$], 1414.8 [$11/2^-$,$9/2^-$], (1834.0) [$11/2^-$,$9/2^-$], 1983.1 [$9/2^-$], 2063.5 [$11/2^-$,$9/2^-$], 2091.6 [$11/2^-$,$9/2^-$], 2119.0 [$11/2^-$,$9/2^-$], and 2702.4 keV [$13/2^-$,$11/2^-$,$9/2^-$]. Less than 0.2% of the decay of $11/2^-$ ^{141m}Sm proceeds via an *M*4 isomeric transition to 11.3-min $3/2^+$ ^{141g}Sm. Two-thirds of the ^{141m}Sm ε decay goes to the six (possible seven) highest-lying states in ^{141}Pm, another example analogous to ^{139m}Nd decay of the population of a well-defined three-quasiparticle multiplet by an *N*=79 nuclide. In simple shell-model terms this can be written as $(\pi d_{5/2})^2(\nu d_{3/2})^{-2}(\nu h_{11/2})^{-1} \rightarrow (\pi d_{5/2})(\nu d_{3/2})^{-1}(\nu h_{11/2})^{-1}$. Most of the remaining states can be characterized quite satisfactorily as specific single-particle and core-coupled states. The behavior of these states allows us to add considerably to the systematics of shell-model orbits and their occupations in this region below *N*=82.

I. PREAMBLE

These results of our study of the decay of $^{141m}_{62}Sm_{79}$ supplement the similar work done on the decay of $^{139m}_{60}Nd_{79}$ by Beery, Kelly, and McHarris.[1] The decay of $11/2^-$ ^{139m}Nd selectively populates six high-spin states at relatively high energies in ^{139}Pr. These states were characterized as three-quasiparticle states having the configuration, $(\pi d_{5/2})(\nu d_{3/2})^{-1}(\nu h_{11/2})^{-1}$, and the preferred ε decay of ^{139m}Nd could be written as $(\pi d_{5/2})^2(\nu d_{3/2})^{-2}(\nu h_{11/2})^{-1} \rightarrow (\pi d_{5/2})(\nu d_{3/2})^{-1}(\nu h_{11/2})^{-1}$.

The work on ^{139m}Nd decay led to the prediction by McHarris, Beery, and Kelly[2] that other N=79 or N=77 nuclides might possess the requisite configurations for similar ε or β^+ decay into three-quasiparticle multiplets. In addition to the configuration such a nuclide must also have sufficient decay energy to populate states above the pairing gap in its daughter, and it must be "hung up" with respect to other modes of decay — for example, if it is a metastable state the energy for the isomeric transition must be low enough to make that transition quite slow.

Working ones way out from β stability, he finds that ^{141m}Sm and ^{137m}Nd are the next likely candidates. For example, the addition of two protons to the ^{139m}Nd configuration produces the very similar configuration for ^{141m}Sm, $(\pi d_{5/2})^4(\nu d_{3/2})^{-2}(\nu h_{11/2})^{-1}$. The calculated Q_ε is more than 5 MeV, allowing it to populate high-lying states in ^{141}Pm. Finally, as in the other N=79 odd-mass isotones, the $h_{11/2} \rightarrow d_{3/2}$ (metastable $\rightarrow$ ground state) separation is small ($\simeq$171 keV) making the $M4$ isomeric transition very slow. The results that we present in this paper do indeed confirm these predictions — a multiplet of six, possibly seven, states lying between 1414.8 and 2702.4 keV in ^{141}Pm receives some 67% of the decay, and they appear to be

three-quasiparticle states similar to those populated by ^{139m}Nd.

Prior to the current investigation very little work had been done on ^{141}Sm, and, in fact, it is doubtful if it had been observed at all prior to 1967. In 1957 an activity reported[3] as ^{141}Sm was assigned a half-life of 17.5 to 22 days, but in 1966 another report[4] concluded that ^{141}Sm must have a shorter half-life, probably less than three days. The first correct identification of ^{141m}Sm seems to have been made at about the same time by Bleyl, Münzel, and Pfinning[5] and by Arl't et al.[6] The results from these studies, primarily just half-life assignments, are essentially in agreement with our results -- we obtain a half-life of 22.1±0.3 min for ^{141m}Sm. In 1969 Hesse[7] published a more complete decay scheme and identified 32 γ rays as belonging to the decay of this nuclide. However, his decay scheme was incomplete and there was some confusion in his not recognizing the presence of 11.3±0.3-min ^{141g}Sm. The latter species was first identified by Eppley[8] and has a decay scheme paralleling that of ^{139g}Nd.[9] Most recently, we presented[10] a preliminary decay scheme of ^{141m}Sm at the Leysin Conference on Properties of Nuclei Far from the Region of Beta-Stability, and Arl't et al.[11] presented an abstract at the same conference in which they recognized the three-quasiparticle nature of the three states in ^{141}Pm that receive the strongest population and in which they report a half-life of 9.5±0.5 min for ^{141g}Sm.

II. SOURCE PREPARATION

Our principal means of producing ^{141}Sm was via the ^{142}Nd(τ,4n)^{141}Sm reaction (Q = -27.3 MeV), although we also produced the isomers indirectly by the ^{144}Sm(p,4n)^{141}Eu $\xrightarrow{\varepsilon}$ ^{141}Sm (Q = -31.2 MeV). This second method was used primarily to enhance the production of ^{141g}Sm in hopes of distinguishing it better from ^{141m}Sm, which is produced in abundance by the first reaction.

For the τ bombardments, 25-mg targets of separated isotope $^{142}Nd_2O_3$ (>90% ^{142}Nd, obtained from Oak Ridge National Laboratory) were bombarded with a 40-MeV τ beam from the MSU Sector-Focused Cyclotron. Typically, a beam current of 0.1-1.0 μA was used for periods of 1-5 min. For the proton bombardments, separated isotope ≈25-mg $^{144}Sm_2O_3$ (95.10% ^{144}Sm, again from ORNL) targets were bombarded with ≈0.5-μA beams of 40-MeV p's from the MSU Cyclotron for periods of ≈1 min. Because of the short half-lives of ^{141m}Sm (22.1 min) and ^{141g}Sm (11.3 min), no chemical separations were made.

The primary means of determining which γ rays were associated with each of the ^{141}Sm isomers was by comparing the relative intensities of the γ rays in four consecutive spectra. Each one represented a 15-min counting interval, with accumulation in the first spectrum starting 2 min after the end of a bombardment. These four 4096-channel spectra were obtained by means of a routing circuit that allowed their successive storage in different parts of the memory of the MSU Cyclotron Laboratory Sigma-7 computer. We thus accumulated data from many targets in each spectrum. A possible problem in the interpretation of the above data arises from the daughter, ^{141}Pm, which has a 20.9-min $t_{1/2}$; however, we have studied[12] the γ-ray spectra

from the decay of this isotope prepared directly via the $^{142}Nd(p,2n)^{141}Pm$ reaction and can identify its peaks readily. Because of the relatively short half-life of ^{141m}Sm and the presence of ^{141}Pm growing in as a decay product, we always began counting a source as soon as practicable after bombardment. Many (≈10-20) bombardments were made for each experiment described below, and the counting for each was made only during that optimum period that minimized contaminants.

III. EXPERIMENTAL RESULTS

A. Half-Life Determinations

The half-lives of ^{141m}Sm and ^{141g}Sm were determined simultaneously with the aid of the MSU Cyclotron Laboratory Sigma-7 computer and a computer code called GEORGE.[13] This allowed the accumulation of 40 successive 4096-channel spectra, each of 2-min duration. A pulser peak was included in each spectrum to allow determination of the proper dead-time correction.

The half-life of ^{141m}Sm was determined independently from the 196.6-, 431.9, and 538.5-keV peaks (cf. next section). The results were then averaged to yield a value of 22.1±0.3 min. (The spectra and half-life curves can be found in Ref. 8.) The half-life of ^{141g}Sm was determined from the 403.9-keV peak (the only strong, clearly resolved line that belongs to ^{141g}Sm), and the result obtained was 11.3±0.3 min.

B. γ-Ray Singles Spectra

Two Ge(Li) detectors were used to cross-check each other in making energy and intensity measurements on the ^{141m}Sm γ rays. These were a five-sided coaxial detector having 2.5% efficiency (at 1332 keV compared with a 3×3-in. NaI(Tl) detector, source distance 25 cm) and a true coaxial detector having 10.4% efficiency. Under typical operating conditions, using a cooled FET preamplifier, an *RC* linear amplifier with near-Gaussian shaping and DC-coupled base-line restoration, and 12- or 13-bit ADC's coupled to a PDP-9 or Sigma-7 computer, we achieved a resolution of ≈2.2 keV FWHM for the ^{60}Co 1332-keV peak.

The energies of the prominent ^{141m}Sm γ rays were determined by counting the ^{141}Sm source simultaneously with several well-known calibration standards. Above 800 keV, ^{56}Co was the principal standard,[14] while at lower energies ^{54}Mn, ^{57}Co, ^{141}Ce, ^{137}Cs, ^{207}Bi, and ^{243}Cm (cf. Ref. 8) were used. A number of spectra were taken, and the energies of the stronger ^{141m}Sm γ rays were obtained from the average values. These peaks were then used to determine the energies of the weaker ^{141m}Sm γ rays, which were obscured by the standards. The relative intensities were determined by correcting the net peak areas by using a previously prepared efficiency curve. For more details on the methods of data reduction used, cf. Refs. 8 or 15. The first and sixth of the successive 5-min singles spectra that were used to determine the energies and intensities and to assign γ rays on the basis of half-life are shown in Figs. 1a and 1b.

On the basis of half-lives and relative intensities we have assigned at least 47 γ rays to ^{141m}Sm decay. The energies and intensities of these are listed in Table I, where they are compared with the results obtained by Hesse.[7] The two sets of data are in fair agreement, but we see many weak transitions that he did not observe, and we do not include seven γ rays that he associated with ^{141m}Sm decay.

C. Prompt γ-γ Coincidence Spectra

Several types of prompt coincidence experiments were performed using Ge(Li)-Ge(Li) and Ge(Li)-NaI(Tl) spectrometers. These included two-dimensional "megachannel" coincidence experiments, pair spectra experiments, and anticoincidence experiments.

Details of the two-dimensional coincidence experiment can be found in Refs. 8, 15, and 16, so they will not be repeated. Suffice it to say that the 2.5% efficient Ge(Li) detector and another one having 3.6% efficiency (also 2.0 keV resolution FWHM at 1332 keV) were placed in 150° geometry, with a graded Pb shield placed between them to help prevent scattering from one detector into the other. Coincident events (resolving time, 2τ = 160 nsec) from both sides were processed, and their addresses were listed in pairs on magnetic tape. This yielded a 4096×4096-channel array of prompt coincidence events, which could later be sorted off-line in gated slices. The integrated coincidence spectra from each detector are shown at the top of Fig. 2. Some representative gated spectra are shown in the remainder of Fig. 2 and in Fig. 3; the remaining gated spectra can be found in Ref. 8. In these spectra gates were set on the *X* side (2.5% detector) and the displays were taken from the *Y* side (3.6% detector). A summary of the two-dimensional coincidence results is given in Table II.

The pair (511-keV-511-keV-γ) coincidence spectrum shown in Fig. 4 was obtained with total annihilation absorbers around the sources and the 2.5% Ge(Li) detector placed inside an 8×8-in. NaI(Tl) split annulus.[17] The single-channel analyzer associated with each half of the annulus had its window adjusted to accept only the 511-keV region. A triple coincidence

(2τ = 100 nsec) was required before the fast coincidence unit would generate a gate signal and allow pulses from the Ge(Li) detector to be stored. Thus, only double-escape peaks and peaks due to transitions from levels fed by β^+ decay appear in the spectrum in Fig. 4. The $\gamma^{\pm}$ peak is a measure of the chance contributions to the spectrum.

Finally, to complement the various coincidence spectra, an anticoincidence spectrum was taken, again employing the 2.5% Ge(Li) detector and the 8×8-in. NaI(Tl) split annulus. This spectrum is shown in Fig. 5. The ^{141m}Sm source was placed at the center of the annulus tunnel, with the Ge(Li) detector in one end and a 3×3-in. NaI(Tl) detector at the other end. The Ge(Li) detector was operated in anticoincidence with γ rays above 100 keV in the NaI(Tl) detectors (2τ = 100 nsec). The true-to-chance ratio was ≈100/1. This spectrum enhances those transitions that are not in prompt coincidence with the other γ rays or with β^+ emission. It is particularly useful in placing transitions to the ground state or to a metastable state, providing those transitions are primarily ε fed and not β^+ fed.

A summary of the relative intensities of ^{141m}Sm γ rays in some of the more important coincidence spectra is given in Table III.

D. Delayed Coincidence Spectra

Systematics of this nuclear region suggested the presence of a metastable $\pi h_{11/2}$ state in the daughter, ^{141}Pm. In the earlier work on ^{139m}Nd decay[1] a delayed coincidence spectrum was essential in elucidating the decay to the higher-lying states, so we felt compelled to perform similar experiments here.

We identified this $\pi h_{11/2}$ state as the state at 628.6 keV in ^{141}Pm, and by a straightforward comparison of its *M2* deexcitation with that of the $\pi h_{11/2}$ state at 828.1 keV in ^{139}Pr we estimate its half-life to be ≈400 nsec. This is long enough to obtain useful information using a coincidence resolving time of 100 nsec.

Two types of delayed coincidence spectra were obtained. In the first, shown in Fig. 6, the gate signal was delayed 250 nsec with respect to the linear signal. The result of this is to enhance those transitions that depopulate the state having an appreciable half-life. In the second, shown in Fig. 7, the linear signal was delayed 250 nsec with respect to the gate. Here the result is to enhance those transitions feeding the state having an appreciable half-life. The latter primarily are the transitions that depopulate what we propose as three-quasiparticle states, so this spectrum is crucial in identifying these high-lying, high-spin states.

E. Energy Separation of the Two ^{141}Sm Isomers

Because the ^{141}Sm isomers so admirably meet the requirements of essentially separate decays, it is difficult to determine their energy separation with much precision. Based on a least-squares fit of the previously *measured* *M*4 transitions in the other *N*=79 nuclei, we arrive at an energy of 171.6 keV between the two. An *M*4 transition of this energy, compared with the ε/β^+ half-life, would be expected to be quite weak. The vicinity of 172 keV is a particularly unfortunate region for the observation of a photon of low intensity, since the backscatter peak from annihilation quanta is 170 keV. We have looked for the isomeric transition both in γ-ray and electron spectra without success. An *M*4 transition of this energy should be somewhat easier to see in the electron spectra than in the γ-ray spectra, as the conversion coefficient should be large (≈4, Ref. 18); however, there is no evidence of any transition peaks above the β^+ continuum. Based on the statistics of our γ-ray spectra, we have placed an upper limit of 0.2% of the total ^{141m}Sm decay for this transition. The results of the different investigating groups who have considered the relations between ^{141m}Sm and ^{141g}Sm are summarized in Table IV.

IV. ^{141m}Sm DECAY SCHEME

We have constructed a decay scheme for ^{141m}Sm from a combination of the foregoing prompt and delayed coincidence spectra, aided only incidentally by energy sums and intensities. This decay scheme is presented in Fig. 8 along with the decay scheme[1] of ^{139m}Nd, with which it should be compared. Of the 47 γ rays that we concluded belonged to ^{141m}Sm decay, only six very weak ones could not be placed. All energies are given in keV, and since the presence of ^{141g}Sm in our sources prevented a precise measurement of the ^{141m}Sm β^+ spectra, the Q_ε of ≈5015 keV is a calculated value.[19] The (total) γ-transition intensities are given in percent of the disintegrations of ^{141m}Sm. The β feedings are also given in percent of ^{141m}Sm disintegrations, and they include both the β^+ and ε decay — the surprisingly small β^+ feedings will be discussed below. The energy assigned to each level is a weighted average based on our confidence in the energy precision of the transitions out of that level. In Table V we compare our level scheme with those obtained by Hesse[7] and Arl't et al.[6,11]

The discussion of the construction of this decay scheme will be broken into two parts: discussion of 1) those levels whose mode of decay bypasses the (metastable) 628.6-keV level and 2) those levels that decay primarily through this metastable level.

A. The 196.6-keV and Related Levels

The 196.6-keV transition has been placed as proceeding from the first excited state of ^{141}Pm on the basis of its being the most intense transition in the ^{141m}Sm spectrum. A first excited state at 196.6 keV is completely consistent with the systematics of this region (cf. §VI).

Placement of the 628.6-keV level itself is also straightforward. It decays to ground via the 628.7-keV transition and to the 196.6-keV level via the 431.8-keV transition, as indicated in the prompt coincidence spectra. Expected to be a metastable state on the basis of systematics, this was proven by the delayed coincidence spectra.

Placement of most other levels is not so straightforward and depends on considerable tortuous logic involving the prompt and delayed coincidence spectra. For example, of the eleven γ rays in coincidence with the 196.6-keV γ, only five feed the 196.6-keV level directly. We present only a few crucial points here.

The 804.5-keV level is placed on the basis of a 196.6- and 607.9-keV coincidence and the fact that no γ ray as intense as the 607.9-keV γ was found in the 607.9-keV gated spectrum other than the 196.6-keV γ. Purely on the basis of sums, γ rays at 1029.6 and 1898.0 keV are placed as feeding this level. These are weak transitions that would not show up in the 607.9-keV gated spectrum. Note that the 805.9-keV γ, which feeds the 628.7-keV level, has no relationship to the 804.5-keV level.

Very similar logic, aided by the presence of a 974.1-keV ground-state transition, places the 974.0-keV level. The two levels at 1108.1 and

1983.1 keV are also placed on the basis of the prompt coincidence data, and the placements are corroborated by multiple energy sums and are consistent with the intensities of the interconnecting γ transitions.

The level placed at 837.1 keV is somewhat of a puzzle. The 837.1-keV γ is enhanced in the integral coincidence spectrum and attenuated in the anticoincidence spectrum. There is weak evidence for coincidence with the 196.6-keV γ from inspection of the 837.1-keV gated spectrum. However, there is no enhancement of the 837.1-keV peak in the 196.6-keV gated spectrum. Possibly, Compton events from other peaks (e.g., 875.0-keV) could account for the 196.6-keV peak appearing in the 837.1-keV gated spectrum. With this somewhat conflicting evidence, the 837.1-keV transition has been placed as originating from a level of the same energy. This is substantiated to some extent by the placement of the 577.8-keV γ, which we shall see in the next section fits nicely between the 837.1-keV level and a level at 1414.8 keV that will be placed by coincidence data.

B. The 628.6-keV Level and Spin-Related Levels

The 628.6-keV level is almost certainly a $\pi h_{11/2}$ state. This is demonstrated both by the systematics of the region and by the fact that it has a half-life long compared with the typical resolving times (2τ ≈100 nsec) of the prompt coincidence spectra. That this is in fact the high-spin state is demonstrated by the results of the "delayed gate" coincidence spectrum (Fig. 6). In this spectrum only the peaks at 196.6 and 431.9 keV are present, and that these two transitions are in coincidence is substantiated by the coincidence spectra gated on each one. And further support for the assignment of an isomeric state at 628.6 keV comes from the enhancement of the relatively weak 628.7-keV γ in the anticoincidence spectrum. That ^{141m}Sm is also an $11/2^-$ state means that its primary β^+/ε decay will populate relatively high-spin (9/2, 11/2, 13/2) states in ^{141}Pm and these states should decay by cascades that go through the 628.6-keV state.

The "delayed spectrum" integral coincidence spectrum (Fig. 7) almost immediately places six of the high-lying, high-spin states fed directly by ^{141m}Sm. [This assumes that the six γ rays enhanced in this spectrum feed the 628.6-keV level directly. The absence of sum transitions or observed coincidences and the fact that the resulting decay scheme is the simplest consistent with the experimental data lead us to accept this assumption of direct feeding.] These six levels lie at 1167.2, 1313.2, 1414.8, 2091.6, 2119.0, and 2702.4 keV. In addition to these six levels, we place a level at 2063.5 keV on the basis of sums — the weak 1434.9-keV γ connects this level with the 628.6-keV level. The 2063.5-keV level is confirmed by the coincidence

relations between the 750.3- and 684.6- and between the 896.5- and 538.5-keV γ's.

The remaining level, at 1834.0 keV, is placed only on the basis of energy sums and should thus be considered only tentative.

Numerous corroborations of the placements of most of the states can be found in the coincidence summary of Table II and in the coincidence spectra themselves, Figs. 2 and 3.

V. DISCUSSION

A. The ^{141}Sm Isomers

The odd-mass N=79 isotones actually consist of three-hole states, but to a reasonable first approximation their low-lying states can be treated as single-hole states much in the manner of the N=81 isotones. Among the latter there are now seven known isomeric pairs having $(\nu d_{3/2})^{-1}$ ground states and $(\nu h_{11/2})^{-1}$ metastable states connected by $M4$ isomeric transitions.[20] In Fig. 9 we show the energy spacings between the $(\nu d_{3/2})^{-1}$ and $(\nu h_{11/2})^{-1}$ states and also show the squares of the radial matrix elements, $|M|^2$, for the $M4$ transitions as calculated using Moszkowski's approximations for single-neutron transitions.[21] Both the energies and matrix elements follow a gentle-enough trend that one has reasonable confidence in extrapolated values, providing the extrapolation is not carried too far. (The fact that the values of $|M|^2$ are not constant is discussed in some detail in Refs. 1, 20, and 22.)

The $|M|^2$ values for the five known isomeric transitions in the N=79 isotones are somewhat larger than for those in the N=81 isotones. This would indicate that they are less good "single-particle" transitions than the N=81 transitions. However, they are all indubitably $M4$ transitions and can be described with considerable accuracy as $(\nu d_{3/2})^{-2}(\nu h_{11/2})^{-1} \rightarrow (\nu d_{3/2})^{-3}$. As mentioned in §III.$E$, we were unable to detect the presence of an isomeric transition between ^{141m}Sm and ^{141g}Sm, but its predicted intensity should be so low that one would not expect to observe it. More to the point, the decay properties[9] of ^{141g}Sm make it reasonably certain that it has a $3/2^+$ ground state. (The $\nu s_{1/2}$ state crosses the $\nu d_{3/2}$

state in this vicinity, but a ^{145g}Gd ground state of $1/2^+$ has quite different decay properties[15] from ^{141g}Sm and, in fact, populates three-quasiparticle states somewhat analogous to those populated by ^{139m}Nd and ^{141m}Sm.) Also, the analogy of ^{141m}Sm decay to ^{139m}Nd, where the $M4$ transition was easily measured, gives us reasonable confidence that the primary configuration of ^{141m}Sm is indeed $[(\pi g_{7/2})^8(\pi d_{5/2})^4]_0[(\nu d_{3/2})^{-2}(\nu h_{11/2})^{-1}]_{11/2^-}$ and that of ^{141g}Sm is $[(\pi g_{7/2})^8(\pi d_{5/2})^4]_0[(\nu d_{3/2})^{-3}]_{3/2^+}$.

B. Single-Particle States in ^{141}Pm

For convenience of discussion the states in ^{141}Pm populated by ^{141m}Sm decay can be divided into three classes: 1) single-particle states or states exhibiting appreciable single-particle character, 2) three-particle states, viz., the high-lying multiplet receiving most of the direct β^+/ε population, and 3) the remaining states, most of which appear to contain core-coupled vibrational components. As relatively little has been done in the way of calculations on states in rare-earth nuclei on the neutron-deficient side of N=82, one has to rely rather heavily on parallels with ^{139m}Nd decay and on general systematics of states in this region. As an aid for following the systematics and trends, in Figs. 10 and 11, respectively, we plot the known states in neutron-deficient odd-mass Pm isotopes and in the odd-mass N=80 isotones. Because few reactions studies have been made on nuclei in this region, the number of states reported is very much a function of Q_ε.

Between the closed shells at 50 and 82 the available single-particle orbits are $g_{7/2}$ and $d_{5/2}$ lying relatively close together and then, after a gap of ≈500-1000 keV, $h_{11/2}$, $s_{1/2}$, and $d_{3/2}$ also relatively close together.[30] Systematics as exhibited in Figs. 10 and 11 and extrapolations of the calculations of Kisslinger and Sorensen[31] suggest $5/2^+$ and $7/2^+$ for the two lowest states in ^{141}Pm. As previously pointed out,[32] sixteen nuclei in this region have well-characterized ground states and first excited states with $5/2^+$ and $7/2^+$ or $7/2^+$ and $5/2^+$ assignments. In the Pm isotopes there is a change of ground-state spin between ^{147}Pm and ^{145}Pm, with ^{147}Pm and the heavier isotopes having $7/2^+$ ground states but ^{145}Pm and ^{143}Pm having $5/2^+$ ground states.

Similarly, in the N=80 isotones there is a reversal of these spins between ^{137}La and ^{139}Pr.

In addition to these general arguments, we have three specific arguments for assigning the ground state $5/2^+$ and the 196.6-keV first excited state $7/2^+$. First, the decay properties of ^{141}Pm itself[12] are consistent with a ground state assignment of $5/2^+$ and not $7/2^+$ -- the decay of ^{141}Pm strongly populates the ground state of ^{141}Nd, which has been quite unambiguously characterized[33] as a $(\nu d_{3/2})^{-1}$ state.

Second, since ^{141m}Sm is undoubtedly an $11/2^-$ state, a β transition between it and a $5/2^+$ ground state of ^{141}Pm would have to be at least third forbidden and hence negligibly small. This is consistent with our findings. On the other hand, β decay to a $7/2^+$ first excited state would be first forbidden unique. Although only a small branch would be expected, from the γ-ray intensity balance (including corrections for internal conversion) for this state it appears that as much as 7.6% of the decay might populate it directly, resulting in a log ft ≳7.0. This compares with ≈3% decay[1] from ^{139} Nd to the first excited state in ^{139}Pr with a log ft of ≈7.6. Actually, it would seem reasonable to attribute much of this apparent feeding to errors in the γ-ray intensities and/or to undetected transitions into the state. However, the pair coincidence spectrum (Fig. 4), after correction for chance events and feeding via higher energy states, shows that there is in fact some β^+ decay to the 196.6-keV state. (In both ^{141m}Sm and ^{139m}Nd decays this first forbidden unique transition would involve $\pi g_{7/2} \rightarrow \nu h_{11/2}$, which would be one of the more favorable cases for such a transition, but we would expect the log ft to be greater than 7.0.) Also, in our measurement[8] of the half-life of the 196.6-keV γ we found no evidence for an 11.3-min component, which means that ^{141g}Sm does not populate the 196.6-keV state either directly or indirectly. All of the β feedings are thus consistent with a $7/2^+$ first excited state.

Third, the respective $5/2^+$ and $7/2^+$ assignments are consistent with the branching ratios from the 628.6-keV state, which will be discussed below. We conclude that the ground state of ^{141}Pm is a $5/2^+$ state and the primary component of its wave function is $[(\pi g_{7/2})^8(\pi d_{5/2})^3(\nu d_{3/2})^{-2}]_{5/2^+}$, taken with reference to the closed shells at Z=50 and N=82. Similarly, the primary component of the $7/2^+$ 196.6-keV state is expected to be $[(\pi g_{7/2})^7 \times (\pi d_{5/2})^4(\nu d_{3/2})^{-2}]_{7/2^+}$.

That the 628.6-keV state is the $\pi h_{11/2}$ state {complete configuration of primary component $[(\pi g_{7/2})^8(\pi d_{5/2})^2(\pi h_{11/2})(\nu d_{3/2})^{-2}]_{11/2^-}$} has already been discussed in §III.*D*. The log *ft* of 6.7 for the β^+/ε decay from ^{141m}Sm is on the high side for an allowed transition, but this is entirely reasonable when one examines the particle rearrangements necessary. These are included in the stylized diagram presented in Fig. 12. To first approximation the transition would appear to involve the conversion of a $d_{3/2}$ proton into an $h_{11/2}$ neutron, either directly or perhaps through an intermediate state, plus the simultaneous promotion of the $d_{5/2}$ proton remaining from the pair up into the $h_{11/2}$ orbit. Thus the transition undoubtedly goes by smaller components in the wave functions. That the log *ft* of 6.7 is smaller than that for analogous transition from ^{139m}Nd (there it is 7.0) can be attributed to the $\pi h_{11/2}$ orbit's dropping in energy with increasing Z, thereby providing larger occupations of $h_{11/2}$ proton pairs. Later we shall show that this is consistent not only with ^{141}Sm and ^{141}Pm behavior, but also with the general trends of single-particle states throughout this region.

Since no conversion-electron data are available for transitions following the decay of ^{141}Sm, we show no multipolarity assignments on the decay scheme.

However, the 431.8- and 628.7-keV transitions are expected to be $M2$ and $E3$, respectively. Assuming that the $M2$ transition be retarded to the same degree as the corresponding transition in ^{139}Pr, a factor of about 35, we estimated the half-life of the 628.6-keV state to be 400 nsec. This would lead to a partial half-life for the $E3$ transition of 7.1 μsec. Assuming little or no mixing in the transition, the Weisskopf single-particle estimate[21] for its half-life (neglecting the statistical factor) is 26 μsec. The $M2$ retardation included here is quite reasonable, since $M2$'s are customarily retarded. However, unless the $M2$ is considerably more retarded than we are willing to accept, the $E3$ is *enhanced* over the single-particle estimate, and this enhancement appears to be at least by a factor of 3.6. Although most $E3$'s are retarded, this is now the fifth known $E3$ in this particular nuclear region that is enhanced. The others are in ^{139}Pr, ^{137}La, ^{147}Eu, and ^{149}Eu (Refs. 1, 34, 35, and 36). These all involve similar $h_{11/2}$ states. The simplest explanation is for an octupole core-coupled component of the $5/2^+$ ground state to be admixed into the $11/2^-$ states. Unfortunately, the positions of octupole states in neighboring even-even nuclei are not known, and a more quantitative persual of the problem must await such information.

We do not see any states populated by ^{141m}Sm decay that we can identify with the $\pi d_{3/2}$ or $\pi s_{1/2}$ single-particle orbits, nor could we expect to do so. Even from the decay[9] of ^{141g}Sm it is difficult to associate these orbits with particular states in ^{141}Pm. Both appear to be fractionated and have their strength spread out over many states.

C. A Three-Quasiparticle Multiplet in ^{141}Pm

Some 65% of the β^+/ε decay from ^{141m}Sm populates the multiplet of six states at 1414.8, 1983.1, 2063.5, 2091.6, 2119.0, and 2702.4 keV. (There are seven states if we include the one at 1834.0 keV, which receives about 2% of the population; however, this state is only tentatively placed and thus omitted from the present discussion.) The log ft values range from 5.7 to 6.6, implying that these are all allowed transitions; in fact, they are faster transitions than the $11/2^- \rightarrow 11/2^-$ transition populating the 628.6-keV state.

The explanation for this superficially peculiar behavior of ^{141m}Sm is actually quite straightforward and has been anticipated in the Preamble. It is given in stylized form in Fig. 12. This multiplet of high-spin, high-lying states is a three-quasiparticle multiplet that the rather unique structure of ^{141m}Sm forces it to populate. ^{141m}Sm, three neutron holes below the N=82 closed shell, undoubtedly has as its primary structure, $[(\pi g_{7/2})^8(\pi d_{5/2})^4(\nu d_{3/2})^{-2}(\nu h_{11/2})^{-1}]_{11/2^-}$, as depicted in Fig. 12 and discussed in §V.A. Because of its large Q_ε it can easily populate states in ^{141}Pm above the pairing gap(s). Now, the most probable form of β transition, given the above structure,is $\pi d_{5/2} \rightarrow \nu d_{3/2}$, resulting in the structure, $[(\pi g_{7/2})^8(\pi d_{5/2})^3(\nu d_{3/2})^{-1}(\nu h_{11/2})^{-1}]_{J^-}$, or more simply, $[(\pi d_{5/2})(\nu d_{3/2})^{-1}(\nu h_{11/2})^{-1}]_{J^-}$. Here J^- can be anything from $3/2^-$ to $19/2^-$, but for allowed transitions is limited to $9/2^-$, $11/2^-$, or $13/2^-$. As can be seen from Fig. 8, the analogy with ^{139m}Nd's populating six similar three-quasiparticle states is striking. Some examples of narrowing down the spin assignments follow.

The 1983.1-keV state is the only one that populates anything lower-lying than the $11/2^-$ 628.6-keV state, and, in fact its 1786.4-keV transition to the $7/2^+$ 196.6-keV state is its strongest mode of deexcitation. The only J^π assignment consistent with this is $9/2^-$. We shall see later (after assigning the 974.0- and 1108.1-keV states) that all three γ transitions depopulating this state are most likely *E*1, which *could* be in agreement with the branching ratios. However, we shall not dwell too much on γ-ray branching ratios when speaking of the transitions involving the three-quasiparticle states. By their very nature these states are quite different in structure from the lower-lying states; thus, most γ transitions will proceed primarily via small admixtures in the wave functions, and consequently the branching ratios can be very misleading. For a rather striking demonstration of this the reader is referred to ^{139}Pr (Ref. 1), where many of the multipolarities could be assigned on the basis of conversion coefficients. There it was almost the rule rather than the exception for γ transitions between and out of the three-quasiparticle states to differ from single-particle predictions by orders of magnitude.

Assignments for four of the remaining five states, at 1414.8, 2063.5, 2091.6, and 2119.0 keV, can be narrowed down to $9/2^-$ or $11/2^-$. All except the 2063.5-keV state decay to the 628.6-keV state, indicating some similarities in their wave functions with it, and all four of them also decay to at least one other state that is (or will be in the next section) assigned $9/2^+$ as its highest possible spin. Assignments of $13/2^-$ would force these branches to be *M*2 transitions, not likely to compete even with retarded *M*1's to the $11/2^-$ states.

After our finding the three-quasiparticle multiplet in ^{139}Pr,

it seemed worthwhile to perform a shell-model calculation for the states in the multiplet, using as simple and truncated a basis set as possible. This was carried out by Muthukrishnan and Kromminga,[37] who calculated negative-parity states in ^{139}Pr using only the two configurations, $[(\pi d_{5/2})(\nu d_{3/2})^{-1}(\nu h_{11/2})^{-1}]$ (the basic three-quasiparticle configuration), and $[(\pi h_{11/2})(\nu d_{3/2}{}^{-2})]$ (the basic configuration of the 821.9-keV metastable state in ^{139}Pr). Using an exchange mixture postulated by True, they obtained excellent results for energy predictions agreeing with the experimental positions. There was still some problem, however, with transition probabilities, and it appears that configurations of the sort, $[(\pi d_{5/2})^2(\pi g_{7/2})^{-1}(\nu d_{3/2})^{-1}(\nu h_{11/2})^{-1}]$, will have to be added to the basis set. This can be seen empirically by the gradations in the properties of the states of the three-quasiparticle multiplets both in ^{139}Pr and ^{141}Pm, e.g., the γ transitions directly to the $7/2^+$ first-excited states. The main point is that calculations that intentionally used a truncated basis set give approximately correct answers for the three-particle states in ^{139}Pr. We are presently beginning calculations for ^{141}Pm using both oversimplified and more realistic basis sets and expect similar results.

D. The Remaining States in ^{141}Pm

The structures of the remaining six states, at 804.5, (837.1), 974.0, 1108.1, 1167.2, and 1313.2 keV, are not so straightforward and appear to lie somewhere between the single-particle and the three-particle states. They can perhaps be described best as weakly core-coupled states. Their wave functions would thus contain many components, which partly explains why the three-particle states decay down through many of them. It would also be consistent with the γ-ray branching ratios depopulating them and with the fairly large log ft values for the β^+/ε transitions feeding them. Although not completely conclusive, there is evidence that the 2^+ one-phonon quadrupole vibrational state lies at ≈770 keV in both of the adjacent even-even nuclides, ^{142}Sm and ^{140}Nd (Refs. 38 and 39), quite in line with those in the lighter N=80 even-even isotones. Thus, the energies of the six ^{141}Pm states are in the right range for core-coupled states, the lower ones probably involving the $d_{5/2}$ or $g_{7/2}$ single-particle states and the upper ones the $h_{11/2}$ state.

The 804.5-keV state (log ft =8.6) appears to be fed by a first-forbidden transition, implying positive-parity assignments from 9/2 to 13/2. (A first-forbidden unique transition would also allow $7/2^+$ and $15/2^+$, but we hesitate to include these because all the log ft's are somewhat high, and it is difficult, if not impossible, to concoct a structure for the state that would allow it to be populated by a relatively fast first-forbidden unique transition.) The $13/2^+$ possibility can be eliminated on the basis of the 607.9-keV γ to the 196.6-keV state, for this would force that transition to be an $M3$. However, neither of the other possibilities can

be eliminated. With the $11/2^+$ assignment the 607.9-keV transition would be a pure $E2$ and with the $9/2^+$ assignment it would be a mixed $M1/E2$. Either way the $E2$ component should be collectively enhanced. In fact, an intelligent guess at the nature of the 804.5-keV state would be that it consists specifically of the $g_{7/2}$ single-particle state coupled to a 2^+ quadrupole core vibration — hence the depopulation solely to the 196.6-keV state. $11/2^+$ or $9/2^+$ is also consistent with the feedings to the 804.5-keV state.

We have been rather cautious about using γ-ray branching ratios to predict J^π assignments except when the structures of the states could be corroborated in other ways, viz., the $\pi h_{11/2}$ state at 628.6 keV. It is instructive here to give an example of how such branching ratios could well be misleading. Of the three possible γ transitions depopulating the 804.5-keV state (ignoring the presence of some low-spin states, which lie below it — known from the decay[9] of ^{141g}Sm), one is present. The missing 804.5-keV transition does not tell us much, and it could be consistent with single-particle estimates. However, the missing 175.9-keV transition to the 628.6-keV state must be an $E1$. And single-particle estimates[21] for this $E1$, a 607.9-keV $M1$, and a 607.9-keV $E2$ yield respective half-lives of 4.6×10^{-14}, 1.1×10^{-13}, and 1.5×10^{-10} sec. Obviously the $E1$ is severely retarded over such estimates. With our inferred structures for the 804.5- and 628.6-keV states this retardation is quite understandable, even expected. However, wrong conclusions could easily have come out of blindly applying these "external" selection rules.

The 837.1-keV state, if correctly placed (cf. §IV.*A*), must be a $9/2^+$ state, probably a coupling of a $d_{5/2}$ single-particle state with the

2^+ core. The log ft implies a first-forbidden transition, and the γ transition to the ground state eliminates the $13/2^+$ and $11/2^+$ possibilities.

Similar logic, involving feedings both into and out of the 974.0-keV state allows us to assign it $9/2^+$.

Within the limits of our γ-ray intensities there is no β feeding to the 1108.1-keV state. The γ transitions into it from above, most specifically the 875.0-keV γ from the $9/2^-$ 1983.1-keV state, limit its J^π to $5/2^-$, $7/2^\pm$, $9/2^\pm$, $11/2^\pm$, $13/2^-$ (assuming $E1$, $M1$, or $E2$ multipolarities). Its depopulating γ rays, especially the ground-state transition, further limit J^π to $5/2^-$, $7/2^\pm$, or $9/2^+$. The fact that this state is not populated by ^{141g}Sm decay[9] is a *weak* argument against the $5/2^-$ assignment, but we cannot justify eliminating it completely. Also, the internal structure of this state is probably the least certain in the decay scheme.

The states at 1167.2 and 1313.2 keV exhibit similar properties. The log ft's of 6.9 and 7.0 could mean either allowed or first-forbidden (non-unique) decay. The implied J^π assignments would be $13/2^\pm$, $11/2^\pm$, or $9/2^\pm$. The γ-ray feedings into them from the three-quasiparticle states do not allow any narrowing down of these values. And each state decays by a single γ ray to the 628.6-keV state, again allowing no reduction in the possibilities. It is tempting to think of these states as couplings of the $h_{11/2}$ single-particle state to a 2^+ core. They lie at approximately the expected energies and such a configuration would explain why even with a $9/2^-$ assignment there would be no γ branching to the 196.6-keV or ground state. Also, with such a structure, there should be considerable configuration mixing with the three-particle states (cf., e.g., Ref. 37), which would explain why the log ft's are only slightly higher than the log ft for β^+/ε decay to the 628.6-keV state itself. Thus, we prefer the negative parity options.

E. ε/β^+ Ratios and Corrected log *ft* Values

Straightforward ε/β^+ ratios as calculated by the methods of Zweifel[40] are not in good agreement with the ratios obtained from the pair coincidence spectrum (Fig. 4). This spectrum shows that the 196.6-, 403.9-, and 438.2-keV transitions (the latter two resulting from ^{141g}Sm decay) are the only ones to receive significant β^+ decay. Now, as the calculated ratios are for "simple" allowed transitions, it is expected that the β^+ components will be much smaller for the first-forbidden transitions. However, it is now becoming apparent that hindrances even to an allowed transition usually reduce the β^+ component much more rapidly than the ε component.[15] Thus, the rearrangement depicted in Fig. 12 for the decay to the $\pi h_{11/2}$ 628.6-keV state would be expected to result in the ε/β^+ ratio being larger than the calculated value. (Note, however, that because of the half-life of this state the pair coincidence spectrum would pick up only a small component of its β^+ feeding.) The log *ft* values presented on the decay scheme itself are so-called "normal" values, obtained using the calculated ε/β^+ ratios. We used these for ease of later improvements and corrections and also because most people are more familiar with decay scheme logic based on such values. In Table VI we compare these with the log *ft* values we obtained assuming only ε decay. The latter are expected to be more realistic. Unfortunately, very little has been done on the quantitative theory of ε/β^+ ratios, but we are beginning an investigation of this problem.[41]

VI. CONCLUSION — MAPPING OF SHELL-MODEL ORBITS VIA β DECAY OF NUCLIDES FAR FROM STABILITY

The decay schemes of ^{141m}Sm and ^{139m}Nd, presented in Figure 8, are remarkably similar. However, there are some differences, and these differences allow us to glean some important information about the behavior of shell-model orbits in this region of the nuclidic chart below N=82.

The most striking difference between the two is that whereas in ^{139}Pr there are many low-energy apparently enhanced γ transitions between members of the three-quasiparticle multiplet, in ^{141}Pm such transitions are fewer and weaker. Also, the transitions out of the multiplet to lower-lying states appear to be much more retarded in ^{139}Pr than in ^{141}Pm. Actually, this is more or less what one would expect from the known behavior of shell-model orbits in this region. The retardation of transitions down to the 628.6-keV state, for example, is represented in Figure 12. With only $g_{7/2}$ and $d_{5/2}$ proton states occupied, these transitions would be formally two-particle transitions. A $d_{5/2}$ or $g_{7/2}$ proton would have to be converted into an $h_{11/2}$ neutron, either directly or perhaps through an intermediate state, and the remaining member of the pair would have to be promoted up to the $h_{11/2}$ orbit. Thus the transitions must proceed instead via small admixtures in the wave functions. Such happens in ^{139}Pr. It is known, however, both from reactions studies[30] and from the β^+/ε decay of some N=81 nuclei that the $\pi h_{11/2}$ orbit drops rapidly in energy with increasing Z in this region. For example, the log ft values for the $11/2^- \rightarrow 11/2^-$ transitions in ^{141m}Nd → ^{141}Pr, ^{143m}Sm → ^{143}Pm, and ^{145m}Gd → ^{145}Eu are >7.0, 6.7, and 6.2, respectively (Refs. 42, 43, and 20), and the speed of these transitions

should reflect sensitively the occupation of the $\pi h_{11/2}$ orbit by proton pairs. At Sm, specifically ^{141}Sm, it has acquired enough population by proton pairs to allow the γ transitions to proceed via this component and be less retarded than those in ^{139}Pr.

The β^+/ε decay of ^{139m}Nd and ^{141m}Sm to the $\pi h_{11/2}$ states in their daughters is another indicator of occupancy of the $\pi h_{11/2}$ orbit by pairs (cf. the transition in Figure 12). Thus, we would expect the transition to be faster in ^{141m}Sm $\rightarrow$ ^{141}Pm than in ^{139m}Nd $\rightarrow$ ^{139}Pr, quite consistent with our experimental findings.

The decay of ^{141m}Sm thus is important in two respects. 1) Taken by itself it provides information on a whole multiplet of high-lying states in ^{141}Pm. Simple shell-model calculations should provide information on the major components of their wave functions, and a closer scrutiny of the transition probabilities should provide much information about the smaller components. 2) In the context of this region below N=82, it provides corroboration of the systematic population of low-lying three-quasiparticle multiplets by the β^+/ε decay of some of the $11/2^-$ isomers of the N=79 and 77 isotones. One should next look for this behavior from $^{137(m)}$Nd and perhaps $^{143(m)}$Gd. (The increased occupancy of the $\pi h_{11/2}$ orbit by pairs at $^{143(m)}$Gd may enhance the decay to the $\pi h_{11/2}$ state in ^{143}Eu to the extent that the three-quasiparticle states are not populated so strongly.) In a wider context it also shows that the decay of nuclei far from β stability not only can provide significant information on the positions of shell model orbits and on the properties of complex states, but also can provide information about the occupancies of these various orbits, something previosly reserved for reactions studies.

Acknowledgments:

We thank Dr. H. Blosser and Mr. H. Hilbert for their aid in the operation of the MSU Cyclotron. We also thank the other members of the MSU Nuclear Chemistry and Physics Spectroscopy Groups for their aid in data collection and interpretation: Dr. R. E. Doebler, Mr. G. C. Giesler, Mr. K. L. Kosanke, Mr. R. W. Goles, Mr. J. N. Black, Mr. R. B. Firestone, Dr. J. B. Cross, Mr. L. F. Samuelson, and Mr. W. B. Chaffee. Mrs. Peri-Anne Warstler aided us greatly in preparing the manuscript.

References:

[1]D. B. Beery, W. H. Kelly, and Wm. C. McHarris, Phys. Rev. 188, 1851 (1969).

[2]Wm. C. McHarris, D. B. Beery, and W. H. Kelly, Phys. Rev. Letters 22, 1191 (1969).

[3]F. I. Pavlotskaya and A. K. Lavrukhina, Sov. J. Nucl. Ener. 5, 149 (1957).

[4]I. M. Ladenbauer-Bellis, Radiochim. Acta 6, 215 (1966).

[5]H. J. Bleyl, H. Munzel, and G. Pfinnig, Radiochim. Acta 8, 200 (1967).

[6]R. Arl't, B. Baier, G. Musiol, L. K. Peker, G. Pfrepper, Kh. Shtrusnyi, and D. Kristov, JINR, Dubna, Report 21 (1967).

[7]K. Hesse, Z. Phys. 220, 328 (1969).

[8]R. E. Eppley, Ph. D. Thesis, Michigan State University, COO-1779-32 (1970).

[9]R. R. Todd, R. E. Eppley, R. A. Warner, Wm. C. McHarris, and W. H. Kelly, to be published.

[10]Wm. C. McHarris, R. E. Eppley, R. A. Warner, R. R. Todd, and W. H. Kelly, *International Conference on the Properties of Nuclei Far from the Region of Beta-Stability, August 31-September 4, 1970, Leysin, Switzerland -- Proceedings* (CERN, Geneva, Report 70-30, 1970) p. 435.

[11]R. Arl't, G. Beyer, G. Musiol, E. S. Rydina, S. Seidler, and H. Strusny, Ibid., p. 1141.

[12]F. Y. Yap, R. R. Todd, R. A. Warner, W. H. Kelly, and Wm. C. McHarris, Bull. Am. Phys. Soc. 15, 538 (1971); also to be submitted to Phys. Rev.

[13]GEORGE, a data-taking code with live display developed for the MSU Cyclotron Laboratory Sigma-7 computer by P. Plauger.

[14]D. C. Camp and G. L. Meredith, Lawrence Radiation Laboratory, Livermore, Report No. UCRL-92294 (1970); submitted to Nucl. Phys.

[15]R. E. Eppley, Wm. C. McHarris, and W. H. Kelly, Phys. Rev. C 3, 282 (1971), and references therein.

[16]G. C. Giesler, Wm. C. McHarris, R. A. Warner, and W. H. Kelly, Nucl. Instr. Meth. 91, 313 (1971).

[17]R. L. Auble, D. B. Beery, G. Berzins, L. M. Beyer, R. C. Etherton, W. H. Kelly, and Wm. C. McHarris, Nucl. Instr. Meth. 51, 61 (1967).

[18]R. S. Hager and E. C. Seltzer, Nucl. Data 4A, 1 (1968).

[19]W. D. Myers and W. J. Swiatecki, Lawrence Radiation Laboratory, Berkeley, Report No. UCRL-11980 (1965).

[20]R. E. Eppley, Wm. C. McHarris, and W. H. Kelly, Phys. Rev. C 2, 1929 (1970).

[21]S. A. Moszkowski, in *Alpha-, Beta- and Gamma-Ray Spectroscopy*, ed. by K. Siegbahn (North-Holland Publ. Co., Amsterdam, 1965); S. A. Moszkowski, Phys. Rev. 89, 474 (1953).

[22]G. Jansen, H. Morinaga, and C. Signorini, Nucl. Phys. A128, 247 (1969).

[23]J. C. Hill and M. L. Wiedenbeck, Nucl. Phys. A98, 599 (1967); E. Jacobs, K. Heyde, M. Dorikens, J. Demuynck, and L. Dorikens-Vanpraet, Nucl. Phys. A99, 411 (1967).

[24]A. R. Brosi, B. H. Ketelle, H. C. Thomas, and R. J. Kerr, Phys. Rev. 113, 239 (1959).

[25]D. DeFrenne, E. Jacobs, and J. Demuynck, Z. Phys. 237, 327 (1970).

[26]B. Parsa, G. E. Gordon, and W. B. Walters, Nucl. Phys. A110, 674 (1968).

[27]P. Alexander and J. P. Lau, Nucl. Phys. A121, 612 (1968).

[28]R. B. Frankel, Ph. D. Thesis, University of California, Berkeley, Lawrence Radiation Report No. UCRL-11871 (1964); D. B. Beery, W. H. Kelly, and Wm. C. McHarris, to be published.

[29]R. W. Goles, Wm. C. McHarris, W. H. Kelly, and R. A. Warner, Bull. Am. Phys. Soc. 15, 1670 (1970); also, to be published.

[30]B. H. Wildenthal, E. Newman, and R. L. Auble, Phys. Rev. C 3, 1199 (1971).

[31]L. S. Kisslinger and R. A. Sorensen, Dan. Mat.-Fys. Medd. 32, No. 9 (1960).

[32]D. B. Beery, Ph. D. Thesis, Michigan State University (1969).

[33]D. B. Beery, W. H. Kelly, and Wm. C. McHarris, Phys. Rev. 171, 1283 (1968).

[34]J. R. Van Hise, G. Chilosi, and N. J. Stone, Phys. Rev. 161, 1254 (1967).

[35]E. Yu. Berlovich, V. N. Klementyev, L. V. Krasnov, M. K. Kikitin, and I. Yurski, Nucl. Phys. 23, 481 (1961).

[36]R. E. Eppley, Wm. C. McHarris, and W. H. Kelly, Phys. Rev. C 2, 1077 (1970).

[37]R. Muthukrishnan and A. Kromminga, Phys. Rev. C 3, 229 (1971).

[38]H. P. Malan, H. Münzel, and G. Pfinnig, Radiochim. Acta 5, 24 (1966).

[39]V. V. Remaev, Yu. S. Korda, and A. P. Klyucharev, Izv. Akad. Nauk SSSR, Ser. Fiz. 27, 125 (1963).

[40]P. F. Zweifel, Phys. Rev. 96, 1572 (1954); 107, 329 (1957); and presented graphically in C. M. Lederer, J. M. Hollander, and I. Perlman, *Table of Isotopes* (John Wiley and Sons, New York, 1967) 6th Ed., p. 575.

[41]R. B. Firestone and Wm. C. McHarris, in progress.

[42]Ref. 33 and also Wm. C. McHarris, R. E. Eppley, and W. H. Kelly, to be published.

[43]J. Felsteiner and B. Rosner, Phys. Letters 31B, 12 (1970).

Table I. Energies and Relative Intensities of γ Rays From the Decay of ^{141m}Sm

This Work		Hesse (Ref. 7)	
Energy (keV)	Intensity	Energy (keV)	Intensity
108.5±0.3	0.5 ±0.1	---	---
149.1±0.3	0.7 ±0.2	---	---
196.6±0.3	184 ±18	196.5±0.5	260 ±30
247.9±0.2	1.91±0.35	---	---
431.8±0.1	100 ±5	431.7±0.5	100 ±10
538.5±0.3	20.9 ±1.4	538.0±0.5	18 ±5
577.8±0.3	2.2 ±0.6	---	---
583.4±0.3	0.7 ±0.2	---	---
607.9±0.2	2.5 ±0.3	---	---
628.7±0.1	6.6 ±0.20	628.3±0.5	6.8±1.0
648.7±0.3	0.9 ±0.2	---	---
676.8±0.3	3.4 ±0.5	---	---
684.6±0.2	19.6 ±1.5	684.2±0.5	21.8±2.6
704.2±0.3	1.1 ±0.2	---	---
725.7±0.5	3.6 ±0.6	726.3±0.7	9.9±1.7
750.3±0.3	3.9 ±0.60	749.5±0.8	4.6±1.0
764.3±0.3	0.4 ±0.1	---	---
768.2±0.5	0.4 ±0.1	---	---
777.4±0.3	50.3 ±2.0	777.1±0.5	58.2±7.0
785.9±0.1	16.9 ±1.0	785.8±0.5	20.7±2.5
805.9±0.1	8.8 ±1.6	806.0±0.6	10.8±1.6
820.7±0.3	0.4 ±0.1	---	---
837.1±0.2	8.87±0.30	836.7±0.7	11.5±3.0
875.0±0.1	3.1 ±0.1	874.6±0.7	4.6±1.0
882.0±0.3	0.4 ±0.1	---	---
896.5±0.1	3.6 ±0.4	896.2±0.7	5.6±1.5

Table I. - continued.

This Work		Hesse (Ref. 7)	
Energy (keV)	Intensity	Energy (keV)	Intensity
911.3±0.3	22.8 ±0.6	911.1±0.5	26.5±3.5
924.7±0.1	5.7 ±0.8	924.4±0.7	6.9±1.3
952.1±0.2	2.2 ±0.1	---	---
955.4±0.5	1.7 ±0.1	---	---
974.1±0.5	0.5 ±0.1	---	---
983.3±0.3	18.0 ±0.8	982.9±0.5	21.6±3.5
995.8±0.5	0.9 ±0.2	---	---
1009.1±0.4	7.2 ±0.6	1008.3±0.5	10.5±2.0
1029.6±0.6	1.3 ±0.3	---	---
1108.4±0.2	3.1 ±0.3	---	---
1117.6±0.2	8.0 ±0.6	1117.2±0.6	11.1±1.8
1145.1±0.2	21.6 ±0.8	1144.9±0.5	27.5±4.0
1287.6±0.4	0.7 ±0.3	---	---
1380.9±0.6	0.5 ±0.2	---	---
1434.9±0.4	0.9 ±0.3	---	---
1463.4±0.6	4.5 ±0.8	1462.1±0.8	5.4±2.0
1490.3±0.1	22.9 ±1.5	1490.2±0.5	27.4±3.5
1786.4±0.4	27.1 ±1.1	1785.9±0.6	33.6±4.0
1898.0±1.0	0.94±1.15	1898.5±1.2	2.5±1.0
1979.6±0.2	0.99±0.12	1979.2±0.8	1.6±0.7
2073.7±0.2	3.53±1.2	2072.9±0.6	11.8±2.0
---	---	1136.6±0.8[a]	5.2±1.5
---	---	1530.7±1.0[a]	2 ±1
---	---	1879.9±0.8[a]	6.3±1.5
---	---	1966.9±0.8[a]	2.5±1.0
---	---	2281.1±1.0[a]	1.5±0.5
---	---	2302.6±1.0[a]	1.1±0.4
---	---	2582.3±1.0[a]	2.9±0.8

[a]These γ rays could not be identified in the present investigation.

Table II. Summary of $\gamma-\gamma$ Two-Dimensional Coincidence Results for ^{141m}Sm

Gate Energy (keV)	γ-Rays Enhanced (keV)
Integral	196.6, 247.9, 538.5, 577.8, 607.9, 684.6, 750.3, 777.4, 805.9, 837.1, 875.0, 896.5, 911.3, 924.7, 983.3
196.6	431.8, 607.9, 777.4, 875.0, 911.3, 983.3, 1009.1, 1117.6, 1145.1, 1490.3, 1786.4
247.9	538.5
431.8	196.6, (1490.3)[a]
538.5	247.9, 896.5, 924.7
577.8	837.1 (weak)
607.9	196.6
676.7+684.6	(196.6)[a], 750.3, 805.9
750.3	(196.6)[a], 684.6, 858.5[b]
777.4	196.6, 1117.6, 1145.1
785.9	No coincidence in evidence
805.9	684.6
837.1	No coincidence in evidence
875.0	196.6, 911.3
911.3	196.6, 875.0, 983.3
924.7	(196.6)[a], 538.5, (777.4)[a]
952.1	538.5
983.3	196.6, 911.3
1009.1	196.6, 777.4

Table II. - Continued

1117.6	196.6, 777.4
1145.1	196.6, 777.4
1490.3	(196.6)[a]
1786.4	196.6

[a]These intensities are less than expected for these transitions to be in coincidence. They are considered to arise from chance coincidences.

[b]This is not a ^{141m}Sm transition.

Table III. γ-Ray Intensities for ^{141m}Sm Coincidence Experiments

Energy (keV)[a]	Relative Intensities				
	Singles[a]	Anti-Coinc.	Integral Coinc.	196.6-keV Gate	Delayed Integral Coinc.
196.6	100	77.1	60.4	---	5.74
247.9	1.04	1.67	0.98	---	1.67
431.8	54.6	2.32	22.3	53.0	2.32
538.5	11.3	11.3	8.81	---	11.3
577.8	1.22	---	1.30	---	---
607.9	1.38	---	1.79	1.90	---
628.7	3.60	---	---	---	---
684.6	10.6	8.32	7.30	---	8.32
725.7	1.95	---	---	---	---
750.3	2.14	1.55	1.70	---	1.55
777.4	27.4	---	27.4	27.4	---
785.9	9.20	10.2	4.99	---	10.2
805.9	4.78	4.50	3.45	---	4.50
837.1	4.82	---	3.99	---	---
875.0	1.68	---	1.64	1.97	---
896.5	1.95	---	1.33	---	---
911.3	12.4	---	12.6	12.3	---
924.7	3.08	1.67	2.06	---	1.67
952.1	1.20	---	0.82	---	---
955.4	0.91	---	---	---	---
974.1	0.27	---	---	---	---
983.3	9.80	---	8.03	7.96	---
1009.1	3.93	---	4.04	4.46	---
1029.6	0.68	---	---	---	---
1108.4	1.67	---	1.64	---	---
1117.6	4.37	---	3.99	3.97	---
1145.1	11.8	---	12.3	14.1	---
1463.4	2.43	---	---	---	---
1490.3	12.5	17.9	3.30	---	17.9

Table III. Continued.

Energy (keV)	Relative Intensities				
	Singles	Anti Coinc.	Integral Coinc.	196.6-keV Gate	Delayed Integral Coinc.
1786.4	14.6	---	9.78	17.0	---
1898.0	0.51	---	---	---	---
1979.6	0.54	---	---	---	---
2073.7	1.92	---	---	---	---

[a]The errors placed on these values are given in Table I.

Table IV. Published Estimated Relations Between ^{141m}Sm and ^{141g}Sm

Authors	$t_{1/2}(^{141m}\mathrm{Sm})$	$t_{1/2}(^{141g}\mathrm{Sm})$	E_γ (for $M4$)	% $M4$ in decay
Arl't et al. (Ref. 6)	21.5 min	<10 min	215 keV	---
Bleyl, Münzel, and Pfenning (Ref. 5)	23.5 min	≈2 min	≈200 keV	<1%
Arl't et al. (Ref. 11)	22.5 min	9.5±0.5 min	---	---
This work	22.1±0.3 min	11.3±0.3 min	≈171.6 keV	<0.2%

Table V. States in ^{141}Pm Populated by ^{141m}Sm Decay

This Work		Hesse (Ref. 7)		Arl't et al. (Refs. 6 & 11)[a]	
State Energy (keV)	J^π	State Energy (keV)	J^π	State Energy (keV)	J^π
0	$5/2^+$	0	$(5/2^+)$	0	$(5/2^+)$
196.6	$7/2^+$	196.5	$(5/2^+)$	198	$(7/2^+)$
628.6	$11/2^-$	628.3	$(11/2^-)$	629.9	$(11/2^-)$
804.5	$11/2^+,9/2^+$	---	---	---	---
(837.1)	$9/2^+$	---	---	850	$(15/2^+)$
974.0	$9/2^+$	973.6	---	979	$(9/2^+)$
---	---	1033.2	---	---	---
1108.1	$7/2^\pm,9/2^+,(5/2^-)$	1107.6	---	---	---
1167.2	$13/2^{-(+)},11/2^{-(+)},9/2^{-(+)}$	1166.3	---	---	---
1313.2	$13/2^{-(+)},11/2^{-(+)},9/2^{-(+)}$	1312.5	---	---	---
1414.8	$11/2^-,9/2^-$	---	---	---	---
---	---	1759.4	---	---	---
(1834.0)	$11/2^-,9/2^-$	---	---	---	---
1983.1	$9/2^-$	1982.2	$(9/2^-)$	1982.6	b
2063.5	$11/2^-,9/2^-$	---	---	---	---
2091.6	$11/2^-,9/2^-$	2090.6	---	2091.6	b
2119.0	$11/2^-,9/2^-$	2118.5	---	2119.0	$(9/2^\pm,11/2^\pm)$[b]
2702.4	$13/2^-,11/2^-,9/2^-$	---	---	---	---

[a] Ref. 6 did not include the 1982.6- or 2091.6-keV states.

[b] Ref. 11 includes these plus the revised energy for the 2119.0-keV state and also recognizes that these three states are low-spin members of the three-quasiparticle multiplet.

Table VI. Comparison of log ft's Assuming Either the Theoretical ε/β^+ Ratios or All ε Decay

Level energy (keV)	Normal	ε-decay only
196.6	≥7.0	6.4
628.6	6.7	6.1
804.5	8.6	8.2
837.1	7.2	6.8
974.0	6.8	6.4
1167.2	6.9	6.5
1313.2	7.0	6.6
1414.8	6.6	6.2
1834.0	6.9	6.7
1983.1	5.9	5.7
2063.5	6.4	6.2
2091.6	5.8	5.6
2119.0	5.7	5.5
2702.4	6.5	6.3

Figure Captions

Fig. 1. Singles γ-ray spectra for $^{141m(+g)}$Sm taken with a 10.4% efficient Ge(Li) detector. In (*a*) we show the first and in (*b*) the sixth of successive 5-min spectra that were used to assign γ rays on the basis of half-life. Each spectrum represents about 4 h of counting time obtained from repeated bombardments.

Fig. 2. Results from the two-dimensional "megachannel" coincidence experiments. At the top are the integral coincidence spectra obtained by summing all events for each detector. Gates were normally set on the *X* side (2.5% detector) and displays obtained from the *Y* side (3.6% detector). Four of the more important gated slices are shown.

Fig. 3. Nine additional gated slices from the two-dimensional "megachannel" coincidence experiments. (Cf. Fig. 2.)

Fig. 4. Pair coincidence spectrum to show β^+ feedings from ^{141m}Sm decay. The sources, surrounded by total annihilation absorbers, were placed with the 2.5% Ge(Li) detector in the tunnel of an 8×8-in. NaI(Tl) annulus. The two halves of the annulus were gated on the 511-keV region, and a triple coincidence was required to obtain this spectrum.

Fig. 5. ^{141m}Sm anticoincidence spectrum. Both the sources and the 2.5% Ge(Li) detector were placed inside one end of the tunnel of an 8×8-in. NaI(Tl) split annulus, and a 3×3-in. NaI(Tl) detector blocked the other end of the tunnel. The Ge(Li) detector was then operated in anticoincidence with any of the NaI(Tl) detectors. This spectrum enhances primarily ε-fed ground-state transitions and transitions from the 628.6-keV state ($t_{1/2}$ ≈400 nsec).

Fig. 6. *Delayed-gate* integral coincidence spectrum to pick out the transitions *proceeding from* the 628.6-keV state ($t_{1/2}$ ≈400 nsec) in ^{141}Pm. A 250-nsec passive delay was inserted into the gate (taken from one half of the 8×8-in. NaI(Tl) split annulus) side of the coincidence circuit.

Fig. 7. *Delayed-signal* integral coincidence spectrum. To obtain this spectrum the linear signal (from the 2.5% Ge(Li) detector) was delayed by 250 nsec with respect to the gate signal (from one half of the NaI(Tl) split annulus). This spectrum enhances those transitions that *feed into* the 628.6-keV state ($t_{1/2}$ ≈400 nsec) in ^{141}Pm.

Fig. 8. a) Decay scheme of ^{141m}Sm.

b) Decay scheme of ^{139m}Nd from the work of Beery, Kelly, and McHarris[1] shown for comparison.

Fig. 9. Upper: *M*4 transition energies for the *N*=79 and *N*=81 odd-mass isotones. The ^{141}Sm point is a calculated (predicted) one.

Fig. 9. Lower: Values of the squared radial matrix elements for the single-neutron isomeric transitions in the same nuclei.

Fig. 10. The positions of known states in odd-mass Pm isotopes. The data for ^{147}Pm, ^{145}Pm, ^{143}Pm, and ^{141}Pm come from Refs. 23, 24, 25, and this work, respectively, and are all the result of decay scheme studies.

Fig. 11. The positions of known states in odd-mass N=80 isotones. The data for ^{133}I, ^{135}Cs, and ^{137}La are mostly from decay scheme studies and were taken from Refs. 26, 27, and 28, respectively. The ^{139}Pr data are a combination of decay scheme results from Ref. 1 and ^{141}Pr (p,t) results from Ref. 29, and the ^{141}Pm data come from the present work.

Fig. 12. Stylized diagram depicting some of the important β and γ transitions in the ^{141}Sm-^{141}Pm system. Neutrons are represented by squares and protons by circles. The small arrows point out the particles or holes of most interest in each state. The dashed $h_{11/2}$ proton orbit in parenthesis with the $d_{5/2}$ orbit means that we expect the $h_{11/2}$ orbit to have dropped low enough in energy to have acquired some population by proton pairs.

COUNTS PER CHANNEL
CHANNEL NUMBER
10^6
10^5
10^4
10^3
10^2
10^1
500
1000
1500
2000
2500
3000
3500
4000
108.5
149.1
196.6
247.9
324.4(q)
403.9(q)
431.8
438.2
511.0
538.5
577.8
607.9
628.7
661.9(q)
676.8
684.6
704.2
725.7
750.3
764.3
777.4
768.2
805.3
785.9
837.1
858.5(q)
875.0
896.5
911.3
924.7
983.3
995.8
1009.1
1108.4
1117.6
1145.1
1223.3 (141Pm)
1292.7(q)
1434.9
1490.3
1495.6(q)
1600.9(q)
1778.4
1778.8 (28Al)
1979.6
2005.0(q)
2073.7

Fig. 1a

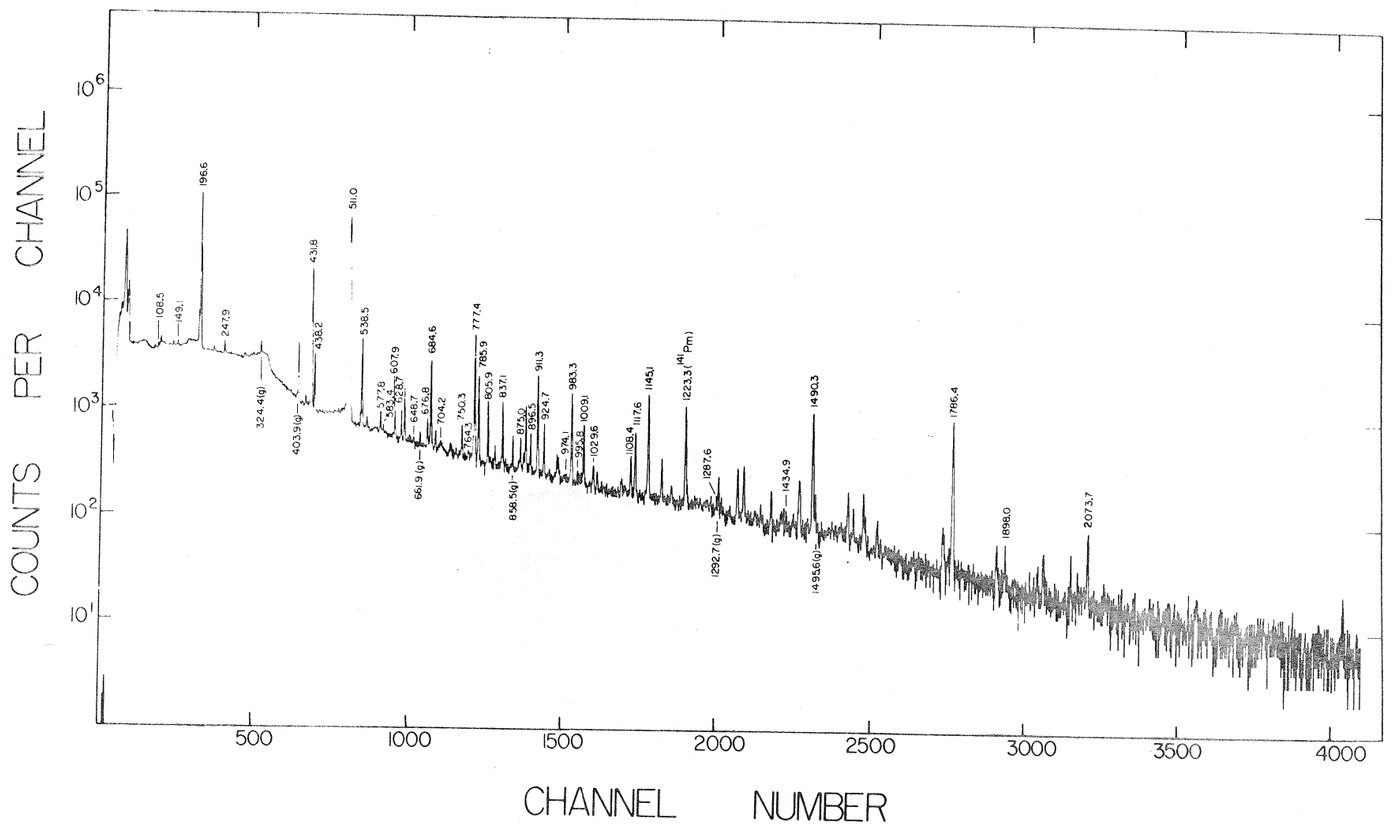
COUNTS PER CHANNEL
CHANNEL NUMBER
196.6
108.5
149.1
247.9
324.4(q)
403.9(q)
438.2
511.0
538.5
684.6
777.4
911.3
983.3
1145.1
1223.3(147Pm)
1434.9
1490.3
1786.4
1898.0
2073.7

Fig. 1b

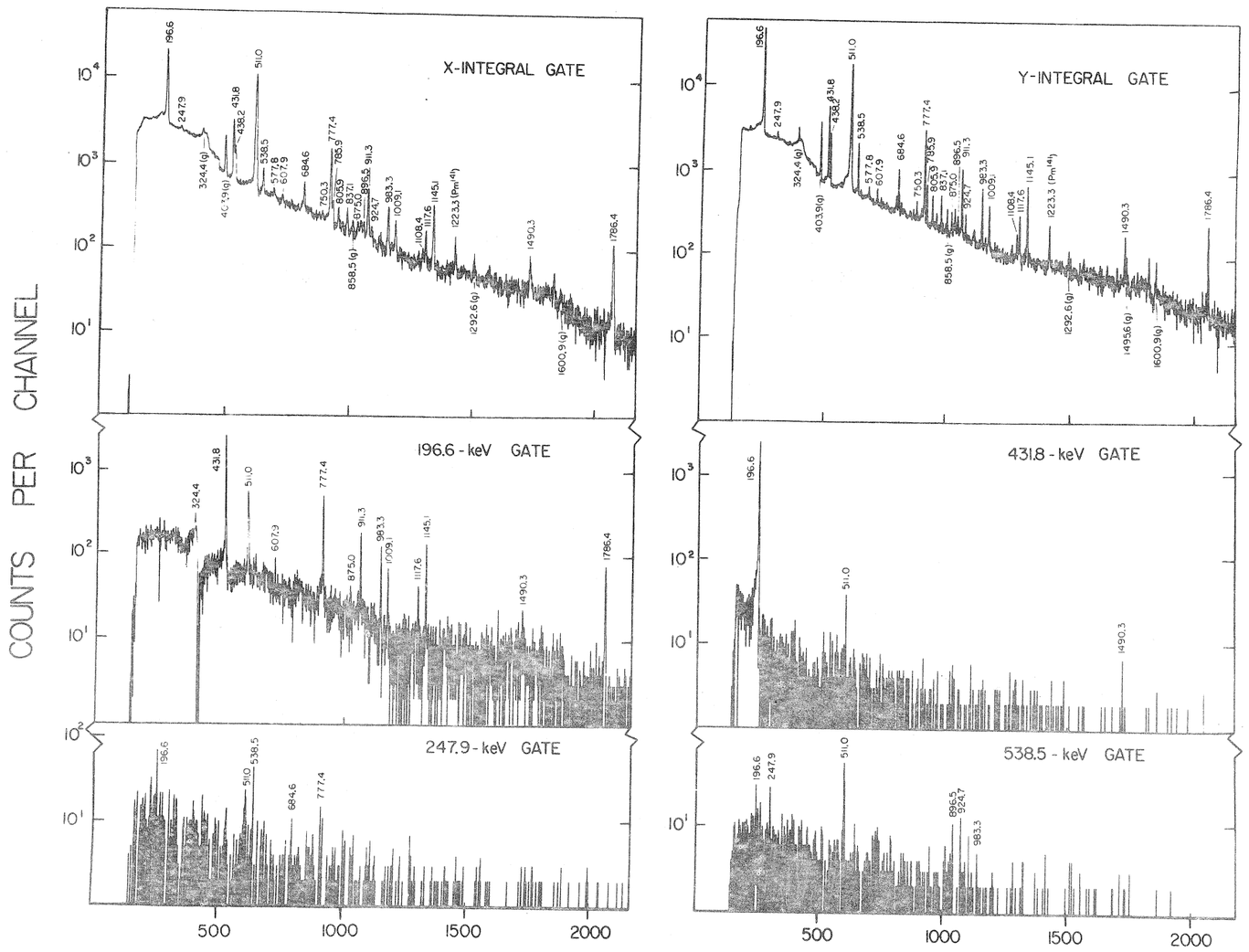
X-INTEGRAL GATE
Y-INTEGRAL GATE
196.6 - keV GATE
431.8 - keV GATE
247.9 - keV GATE
538.5 - keV GATE
COUNTS PER CHANNEL
CHANNEL NUMBER
500
1000
1500
2000

Fig. 2

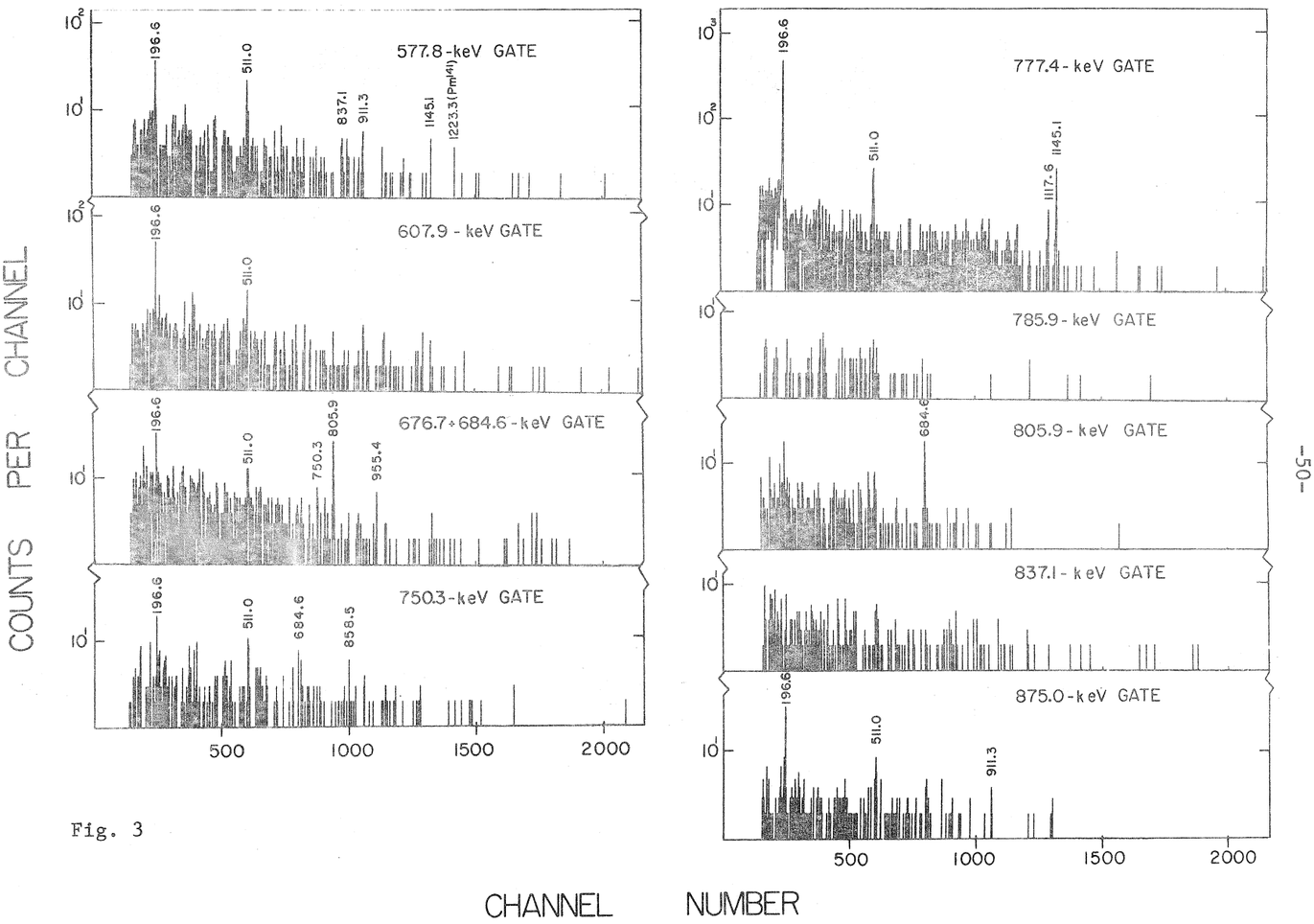
COUNTS PER CHANNEL
577.8-keV GATE
607.9 - keV GATE
676.7+684.6-keV GATE
750.3-keV GATE
777.4-keV GATE
785.9-keV GATE
805.9-keV GATE
837.1-keV GATE
875.0-keV GATE
196.6
511.0
837.1
911.3
1145.1
1223.3(Pm¹⁴⁹)
750.3
805.9
955.4
684.6
858.5
1117.6
500
1000
1500
2000
CHANNEL NUMBER

Fig. 3

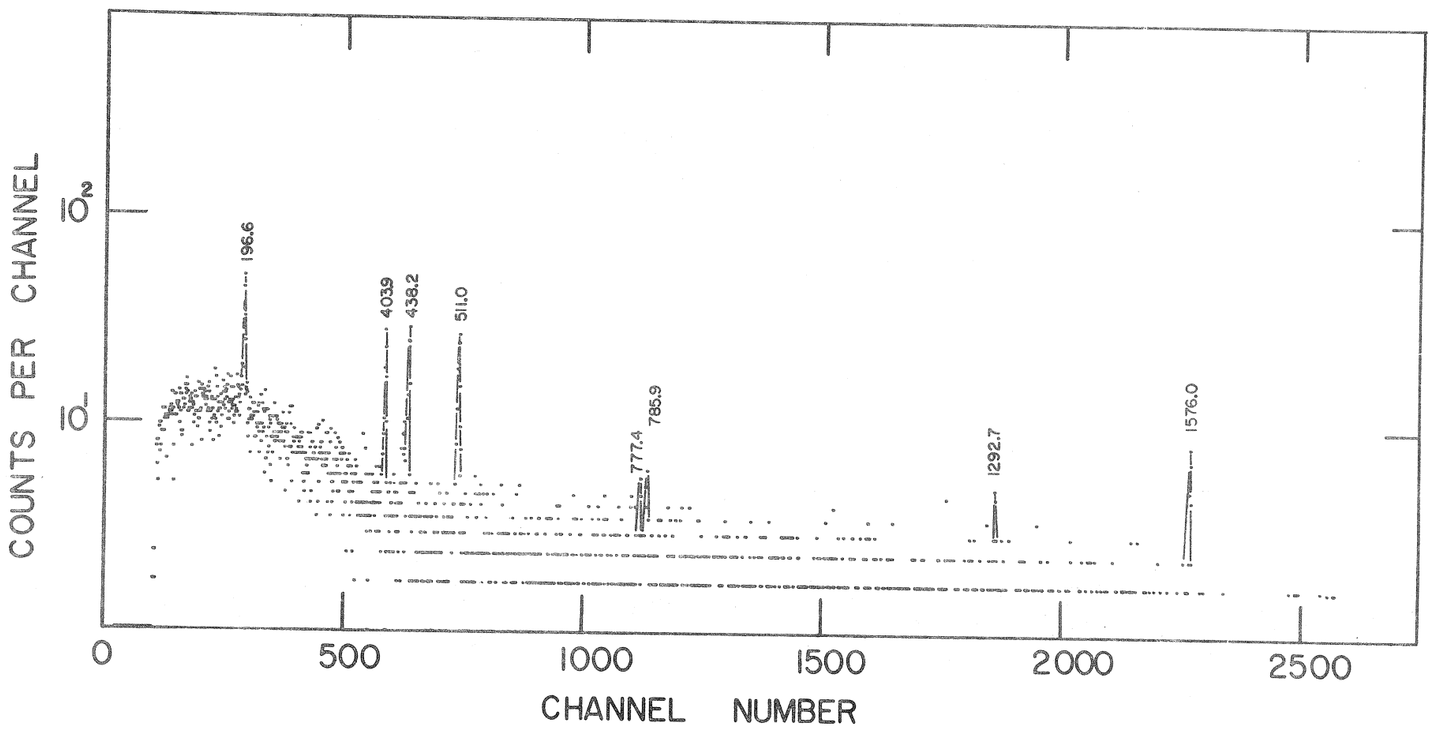
COUNTS PER CHANNEL
$\overline{10}^2$
$\overline{10}$
196.6
403.9
438.2
511.0
777.4
785.9
1292.7
1576.0
0
500
1000
1500
2000
2500
CHANNEL NUMBER

Fig. 4

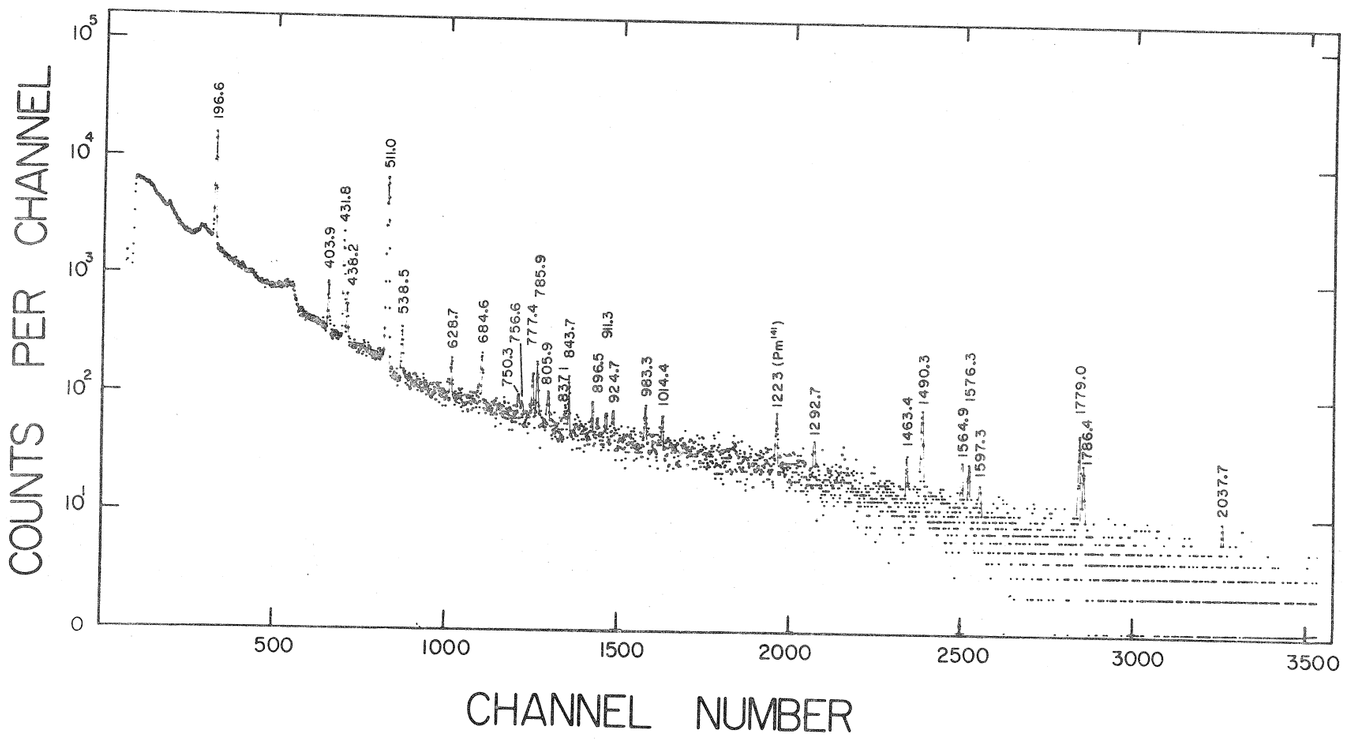
COUNTS PER CHANNEL
CHANNEL NUMBER
196.6
403.9
431.8
438.2
511.0
538.5
628.7
684.6
750.3
756.6
777.4
785.9
805.9
837.1
843.7
896.5
911.3
924.7
983.3
1014.4
1223 (Pm¹⁴¹)
1292.7
1463.4
1490.3
1564.9
1576.3
1597.3
1779.0
1786.4
2037.7

Fig. 5

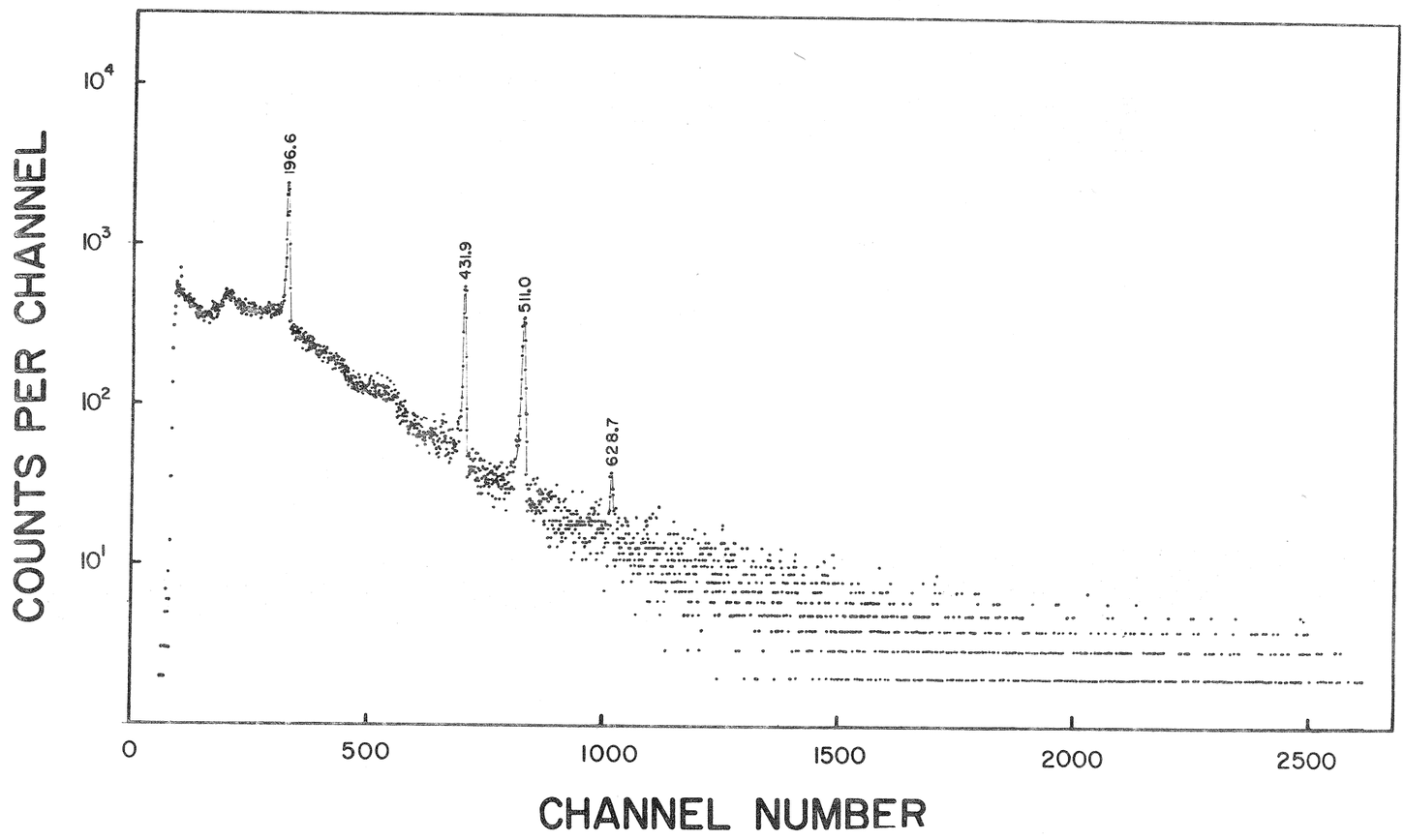
COUNTS PER CHANNEL
10^4
10^3
10^2
10^1
196.6
431.9
511.0
628.7
0
500
1000
1500
2000
2500
CHANNEL NUMBER

Fig. 6

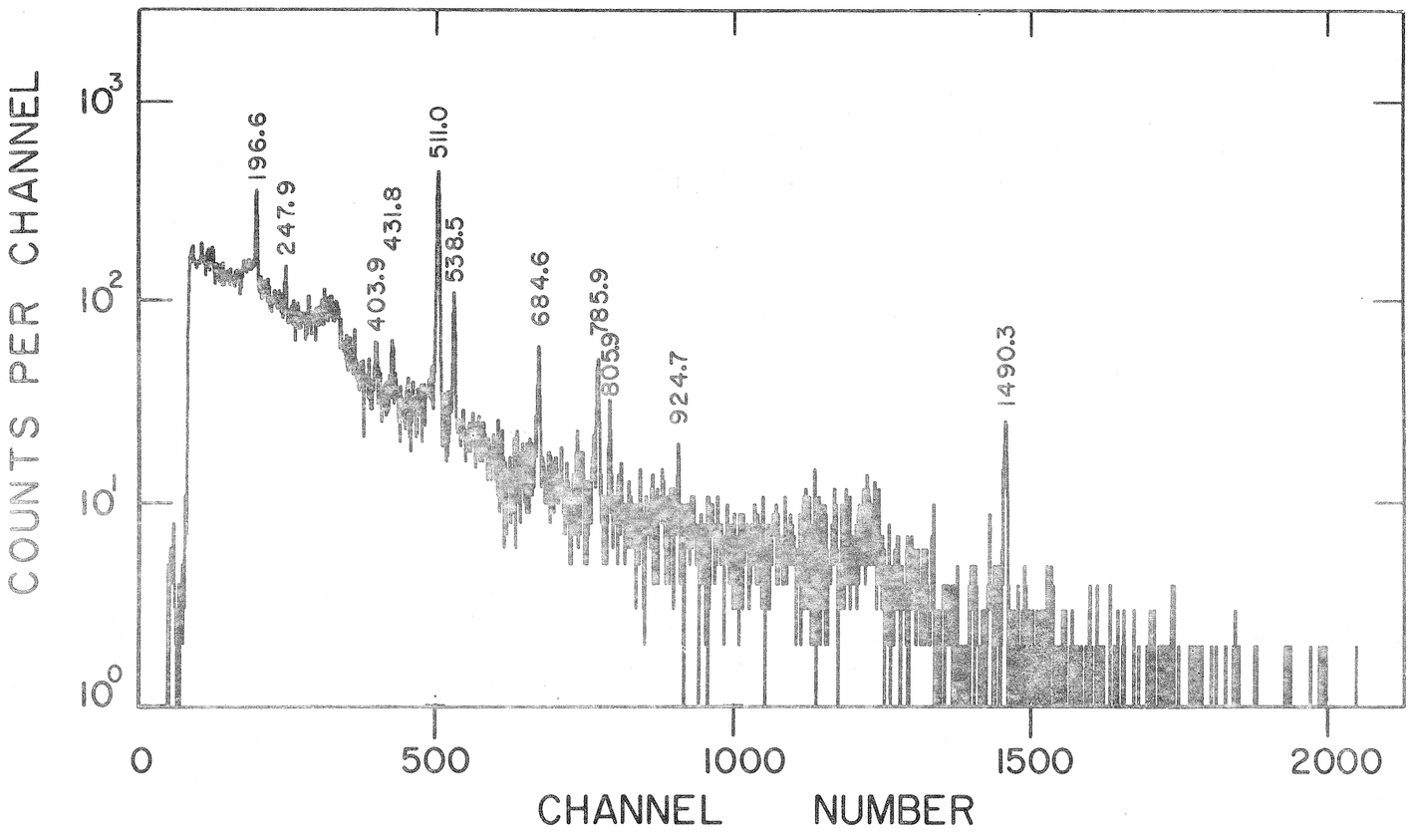
COUNTS PER CHANNEL
10^3
10^2
10^1
10^0
196.6
247.9
403.9
431.8
511.0
538.5
684.6
785.9
805.9
924.7
1490.3
0
500
1000
1500
2000
CHANNEL NUMBER

Fig. 7

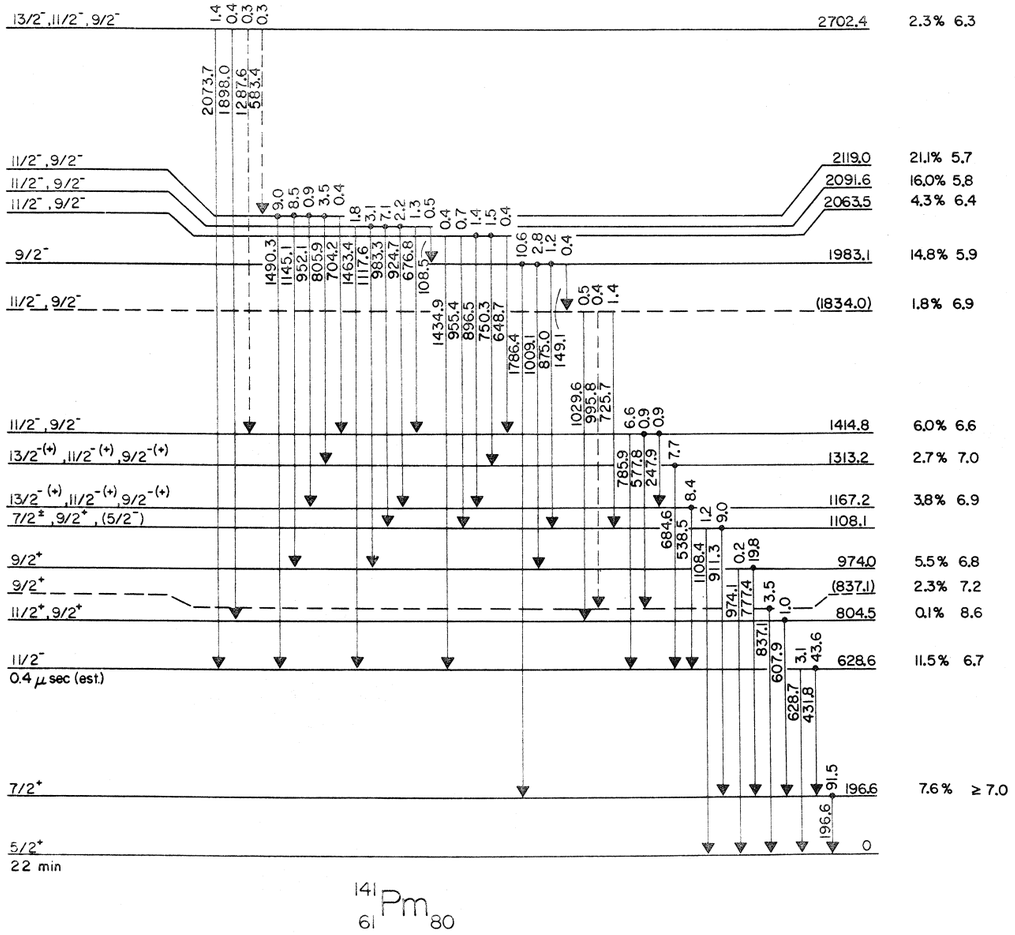
11/2⁻ (≤0.2%) 171 (est.)
22.1 min
3/2⁺ 0
11.3 min
141 62 Sm 79
Q_ε ≈ 5.0 MeV
ε
β⁺
13/2⁻,11/2⁻,9/2⁻ 2702.4 2.3% 6.3
11/2⁻,9/2⁻ 2119.0 21.1% 5.7
11/2⁻,9/2⁻ 2091.6 16.0% 5.8
11/2⁻,9/2⁻ 2063.5 4.3% 6.4
9/2⁻ 1983.1 14.8% 5.9
11/2⁻,9/2⁻ (1834.0) 1.8% 6.9
11/2⁻,9/2⁻ 1414.8 6.0% 6.6
13/2⁻(+),11/2⁻(+),9/2⁻(+) 1313.2 2.7% 7.0
13/2⁻(+),11/2⁻(+),9/2⁻(+) 1167.2 3.8% 6.9
7/2±,9/2⁺,(5/2⁻) 1108.1
9/2⁺ 974.0 5.5% 6.8
9/2⁺ (837.1) 2.3% 7.2
11/2⁺,9/2⁺ 804.5 0.1% 8.6
11/2⁻ 628.6 11.5% 6.7
0.4 μ sec (est.)
7/2⁺ 196.6 7.6% ≥ 7.0
5/2⁺ 0
22 min
141 61 Pm 80

Fig. 8a

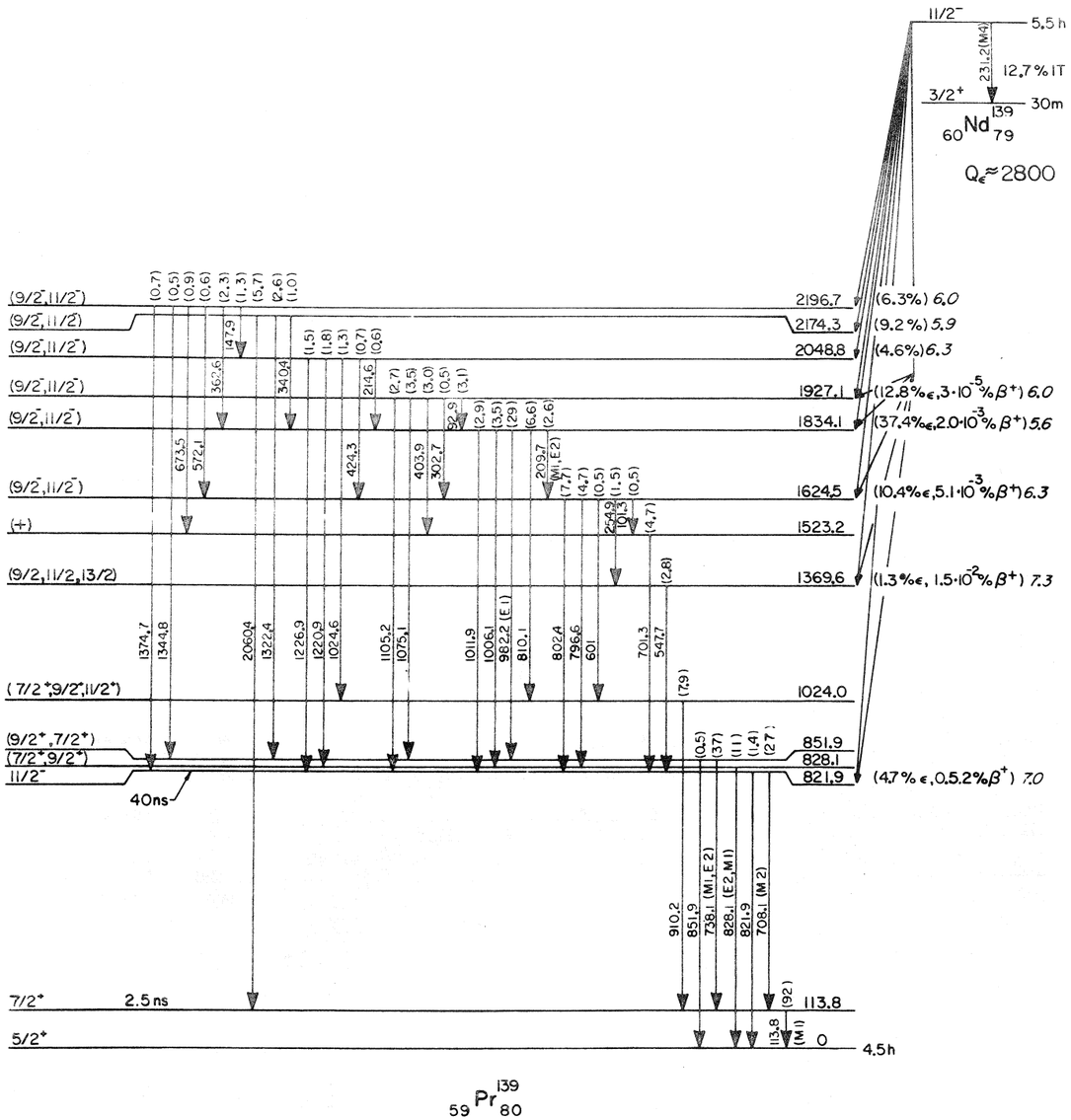
11/2⁻
5.5 h
231.2(M4)
12.7% IT
3/2⁺
30m
60Nd79
Qε≈2800
(9/2⁻,11/2⁻)
2196.7
(6.3%) 6.0
(9/2⁻,11/2⁻)
2174.3
(9.2%) 5.9
(9/2⁻,11/2⁻)
2048.8
(4.6%) 6.3
(9/2⁻,11/2⁻)
1927.1
(12.8%ε,3·10⁻⁵%β⁺) 6.0
(9/2⁻,11/2⁻)
1834.1
(37.4%ε,2.0·10⁻³%β⁺) 5.6
(9/2⁻,11/2⁻)
1624.5
(10.4%ε,5.1·10⁻³%β⁺) 6.3
(+)
1523.2
(9/2,11/2,13/2)
1369.6
(1.3%ε, 1.5·10⁻²%β⁺) 7.3
(7/2⁺,9/2⁺,11/2⁺)
1024.0
(9/2⁺,7/2⁺)
851.9
(7/2⁺,9/2⁺)
828.1
11/2⁻
821.9
(4.7%ε,0.52%β⁺) 7.0
40ns
7/2⁺
2.5 ns
113.8
5/2⁺
0
4.5h
59Pr80

Fig. 8b

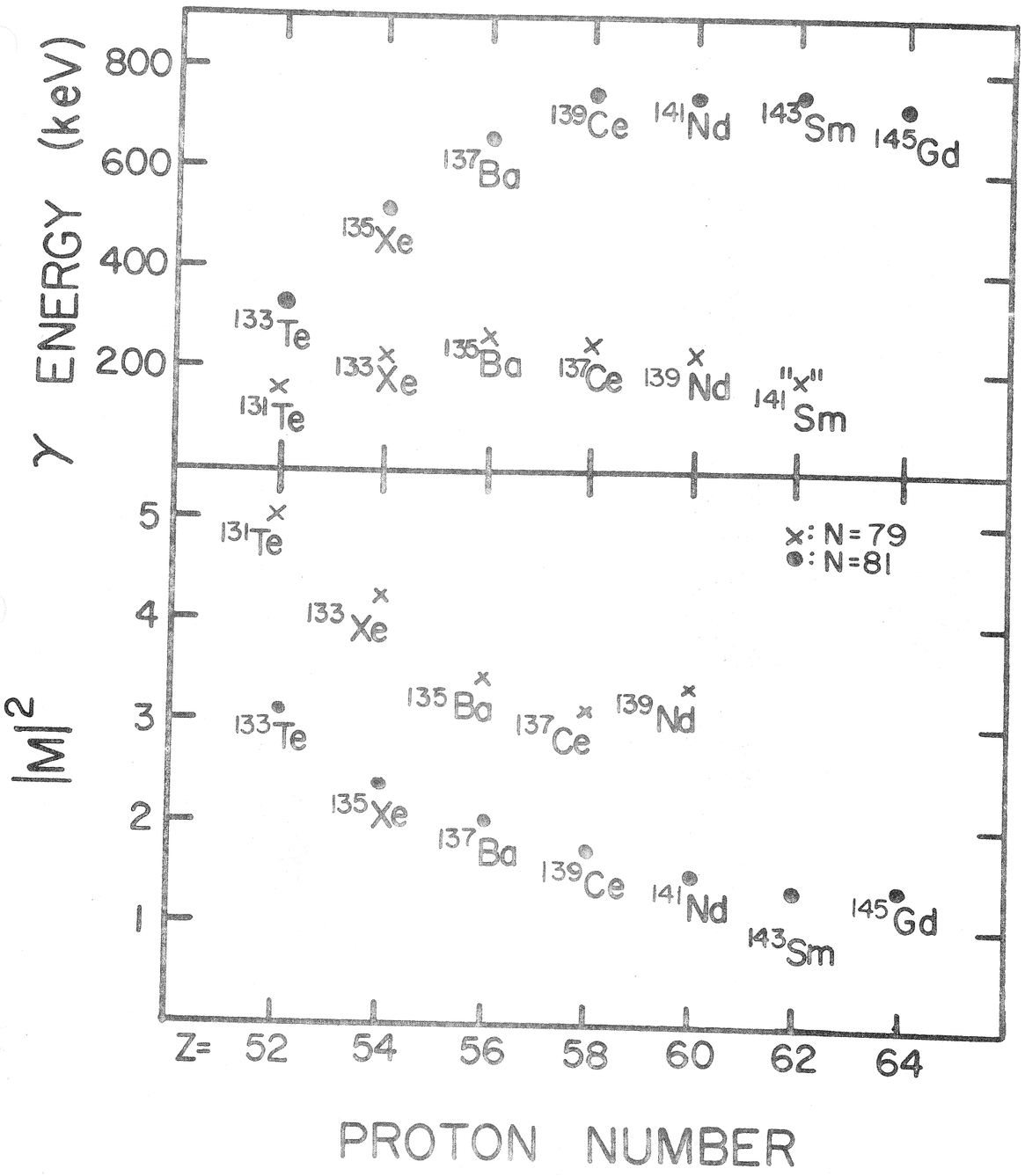
γ ENERGY (keV)
800
600
400
200
5
4
3
2
1
|M|²
139Ce
141Nd
143Sm
145Gd
137Ba
135Xe
133Te
133Xe
135Ba
137Ce
139Nd
141"x"Sm
131Te
131Te
133Xe
135Ba
137Ce
139Nd
133Te
135Xe
137Ba
139Ce
141Nd
143Sm
145Gd
x: N=79
●: N=81
Z= 52 54 56 58 60 62 64
PROTON NUMBER

Fig. 9

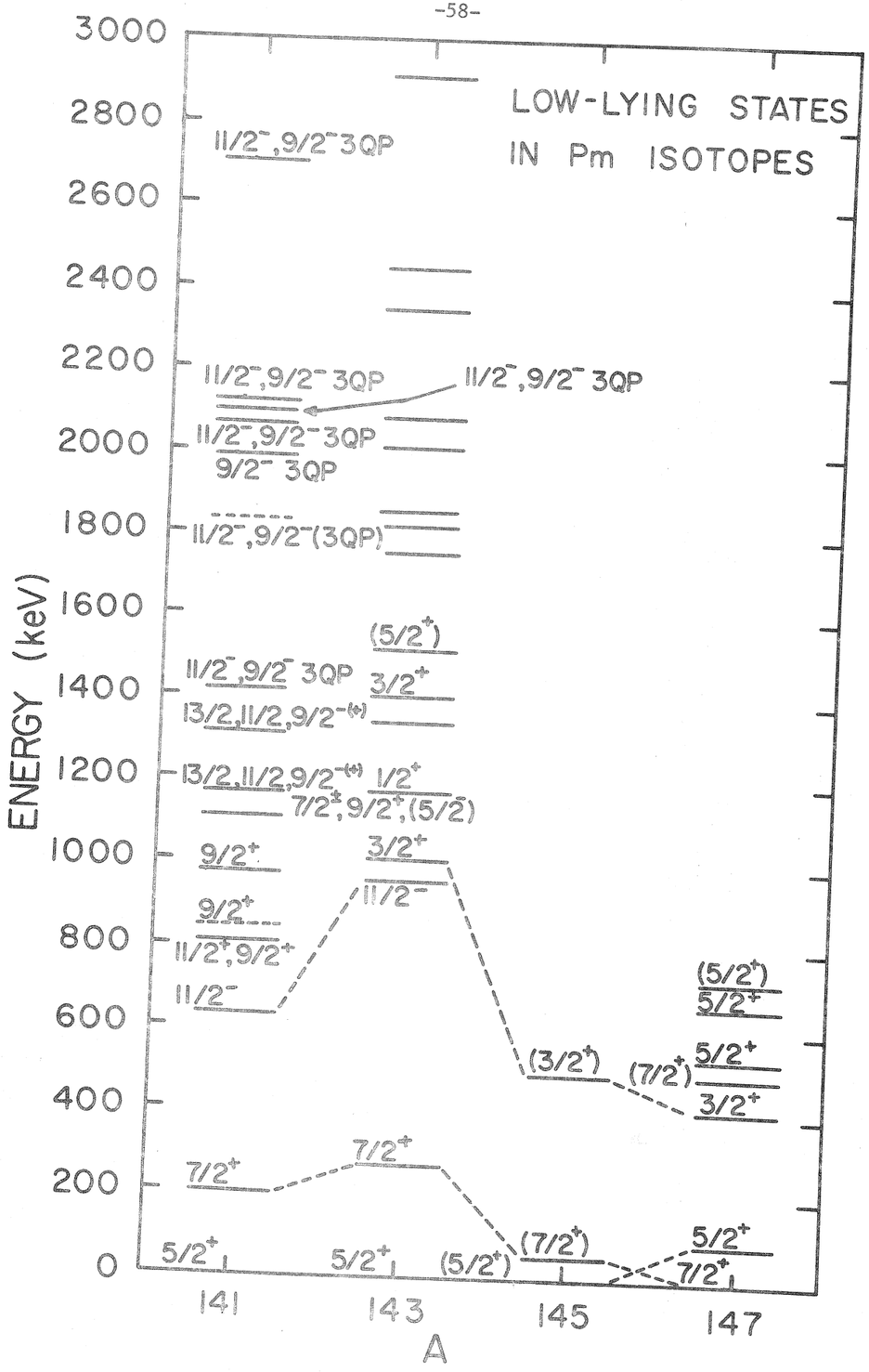
LOW-LYING STATES
IN Pm ISOTOPES
ENERGY (keV)
3000
2800
2600
2400
2200
2000
1800
1600
1400
1200
1000
800
600
400
200
0
11/2⁻,9/2⁻ 3QP
11/2⁻,9/2⁻ 3QP
11/2⁻,9/2⁻ 3QP
9/2⁻ 3QP
11/2⁻,9/2⁻(3QP)
(5/2⁺)
11/2⁻,9/2⁻ 3QP
3/2⁺
13/2,11/2,9/2⁻(*)
13/2,11/2,9/2⁻(*)
1/2⁺
7/2±,9/2⁺,(5/2⁻)
9/2⁺
3/2⁺
9/2⁺
11/2⁻
11/2⁺,9/2⁺
11/2⁻
(5/2⁺)
5/2⁺
(3/2⁺)
(7/2⁺)
3/2⁺
7/2⁺
7/2⁺
5/2⁺
(7/2⁺)
5/2⁺
5/2⁺
5/2⁺
(5/2⁺)
7/2⁺
141
143
145
147
A

Fig. 10

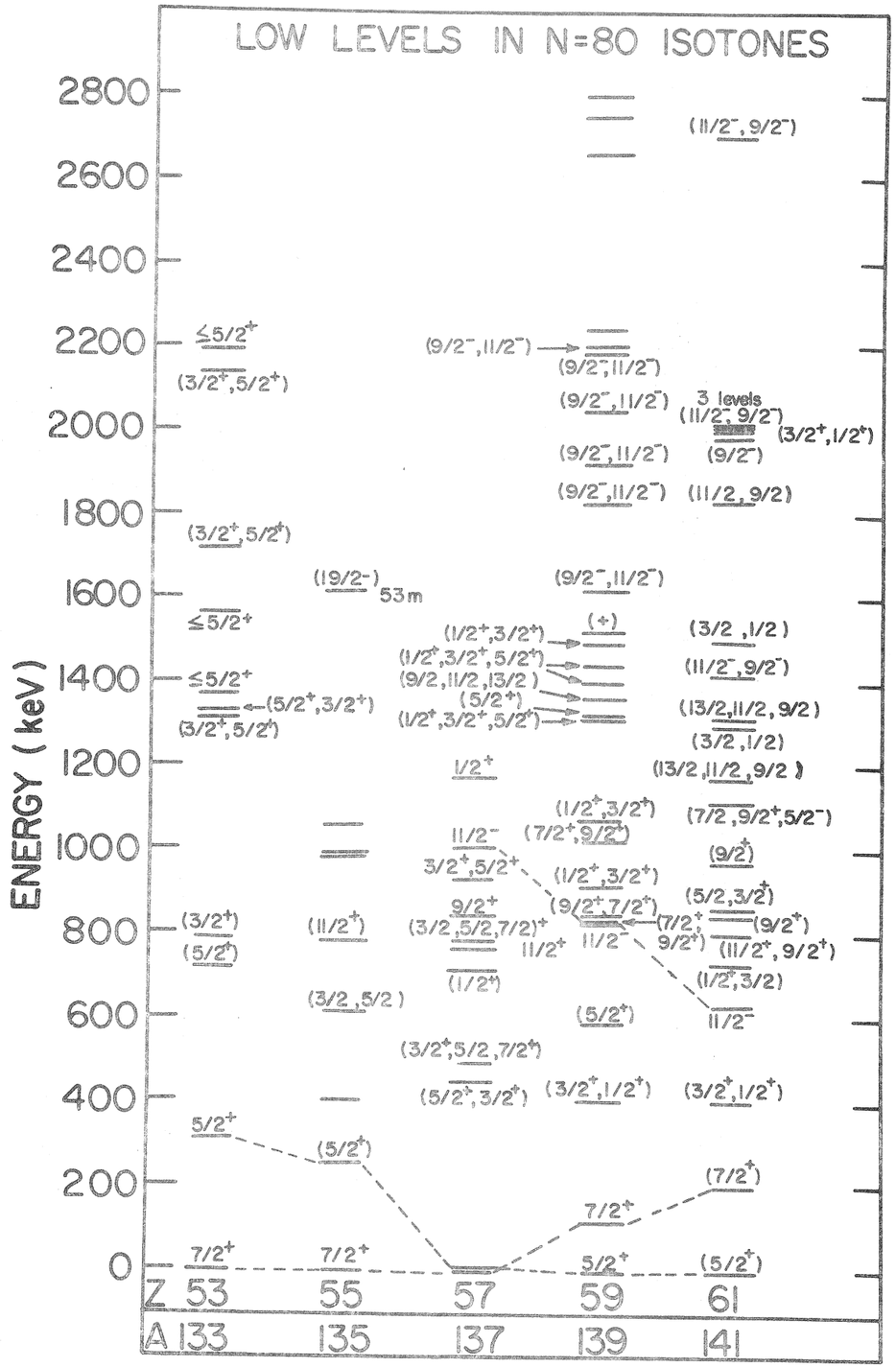
LOW LEVELS IN N=80 ISOTONES
ENERGY (keV)
2800
2600
2400
2200
2000
1800
1600
1400
1200
1000
800
600
400
200
0
Z 53 55 57 59 61
A 133 135 137 139 141
≤5/2+
(3/2+,5/2+)
(3/2+,5/2+)
(19/2-) 53m
≤5/2+
≤5/2+
(5/2+,3/2+)
(3/2+,5/2+)
1/2+
(3/2+)
(5/2+)
(11/2+)
(3/2,5/2)
(3/2+,5/2,7/2+)
(5/2+,3/2+)
5/2+
(5/2+)
7/2+
7/2+
(9/2-,11/2-)
(9/2-,11/2-)
(9/2-,11/2-)
(9/2-,11/2-)
(9/2-,11/2-)
(+)
(1/2+,3/2+)
(1/2+,3/2+,5/2+)
(9/2,11/2,13/2)
(5/2+)
(1/2+,3/2+,5/2+)
11/2-
3/2+,5/2+
9/2+
(3/2,5/2,7/2)+
11/2+
(1/2+)
(5/2+)
(3/2+,5/2,7/2+)
(5/2+,3/2+)
(1/2+,3/2+)
(7/2+,9/2+)
(1/2+,3/2+)
(9/2+,7/2+)
11/2-
(3/2+,1/2+)
7/2+
5/2+
(11/2-,9/2-)
3 levels
(11/2-,9/2-)
(9/2-)
(11/2,9/2)
(3/2,1/2)
(11/2-,9/2-)
(13/2,11/2,9/2)
(3/2,1/2)
(13/2,11/2,9/2)
(7/2,9/2+,5/2-)
(9/2+)
(5/2,3/2+)
(7/2+
(9/2+)
9/2+)
(11/2+,9/2+)
(1/2+,3/2)
11/2-
(3/2+,1/2+)
(7/2+)
(5/2+)

Fig. 11

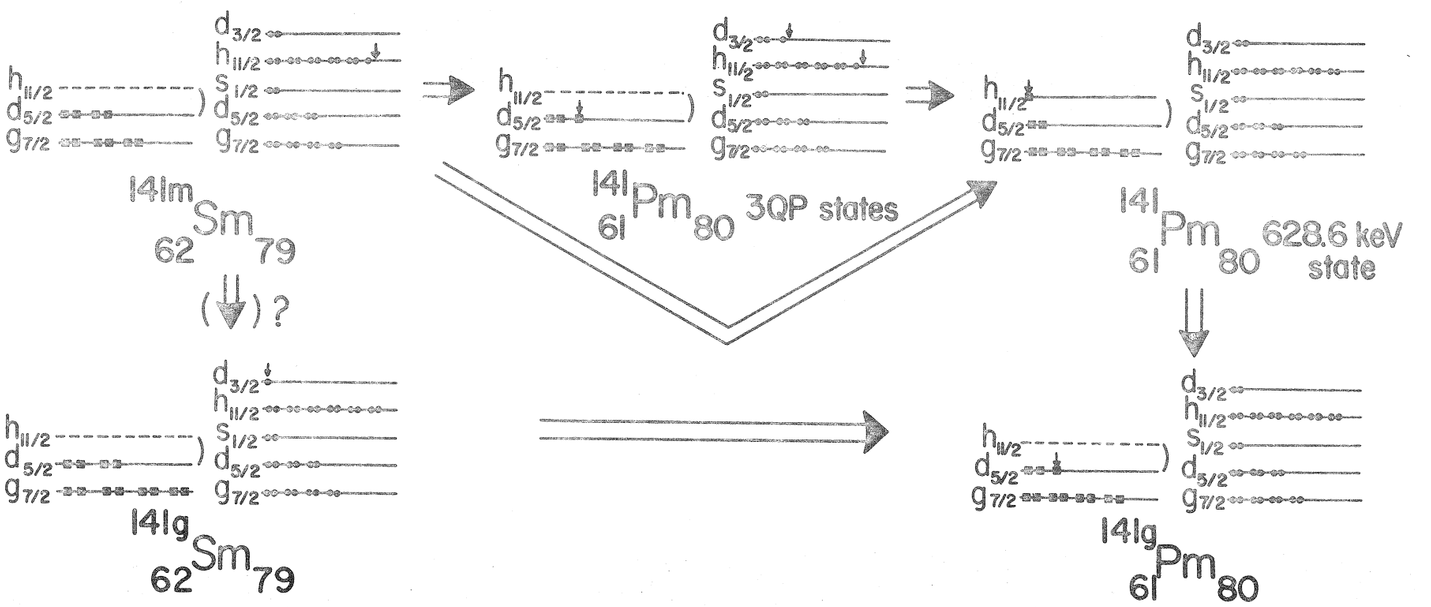
$h_{11/2}$
$d_{5/2}$
$g_{7/2}$
$d_{3/2}$
$h_{11/2}$
$s_{1/2}$
$d_{5/2}$
$g_{7/2}$
141m Sm 62 79
(⇓)?
141 Pm 61 80 3QP states
141 Pm 61 80 628.6 keV state
141g Sm 62 79
141g Pm 61 80

Fig. 12